Short Communication

Validation of uPA/SCID Mouse with Humanized Liver as a Human Liver Model: Protein Quantification of Transporters, Cytochromes P450, and UDP-Glucuronosyltransferases by LC-MS/MS[S]

ABSTRACT

Chimeric mice with humanized liver (PXB mice) have been generated by transplantation of urokinase-type plasminogen activator/severe combined immunodeficiency mice with human hepatocytes. The purpose of the present study was to clarify the protein expression levels of metabolizing enzymes and transporters in humanized liver of PXB mice transplanted with hepatocytes from three different donors, and to compare their protein expressions with those of human livers to validate this human liver model. The protein expression levels of metabolizing enzymes and transporters were quantified in microsomal fraction and plasma membrane fraction, respectively, by means of liquid chromatography–tandem mass spectrometry. Protein expression levels of 12 human P450 enzymes, two human UDP-glucuronosyltransferases, eight human ATP binding cassette (ABC) transporters, and eight human solute carrier transporters were determined. The variances of protein expression levels among samples from mice humanized with hepatocytes from all donors were significantly greater than those from samples obtained from mice derived from each individual donor. Compared with the protein expression levels in human livers, all of the quantified metabolizing enzymes and transporters were within a range of 4-fold difference, except for CYP2A6, CYP4A11, bile salt export pump (BSEP), and multidrug resistance protein 3 (MDR3), which showed 4- to 5-fold differences between PXB mouse and human livers. The present study indicates that humanized liver of PXB mice is a useful model of human liver from the viewpoint of protein expression of metabolizing enzymes and transporters, but the results are influenced by the characteristics of the human hepatocyte donor.

Introduction

Species differences in drug metabolism and transport in the liver between humans and experimental animals are a critical issue during drug development. To overcome this problem, chimeric mice with humanized liver (PXB mice; PhoenixBio Co., Ltd., Hiroshima, Japan) have been generated by transplantation of human hepatocytes into albumin enhancer/promoter-driven urokinase-type plasminogen activator/severe combined immunodeficiency (uPA$^{+/+}$/SCID) mice; in these mice approximately 80% of the hepatocytes are human (Tateno et al., 2004). PXB mice generate human-specific metabolites (Inoue et al., 2009; Kamimura et al., 2010; Yamazaki et al., 2010; De Serres et al., 2011), and pregnane X receptor (PXR)–dependent induction of metabolizing enzymes was observed when the mice were

treated with a human PXR ligand (Hasegawa et al., 2012). Therefore, the liver of PXB mice is considered to be potentially useful as a model of human liver for studies of drug metabolism.

The uptake of most drugs from circulating blood into the liver at the sinusoidal membrane of hepatocytes involves active transport. The drugs subsequently undergo biotransformation by intracellular enzymes such as cytochrome P450 (P450) and UDP-glucuronosyltransferase (UGT), and the parent drug or its metabolites are eventually excreted from the hepatocytes by canalicular and/or sinusoidal transporter proteins. Therefore, expression analyses of metabolic enzymes and transporters in the liver of PXB mice are essential to validate the model. For example, it has been established by means of quantitative PCR and quantitative immunoblot analyses that PXB mice with a high replacement ratio express eight human P450s and human phase II enzymes, including three UGTs, at levels similar to those in human liver (Katoh et al., 2004,2005). Gene expression of the human ATP binding cassette (ABC) transporters and human solute carrier (SLC) transporters was also confirmed in humanized liver (Nishimura et al., 2005; Kikuchi et al., 2010). However, protein expression of drug transporters has not yet been quantitatively analyzed in PXB mice. This is important, because we recently showed that there is a poor correlation between protein and mRNA expression levels of metabolizing enzymes (except

ABBREVIATIONS: ABC, ATP binding cassette; BCRP, breast cancer resistance protein; BSEP, bile salt export pump; CV, coefficient of variance; γ-GTP, γ-glutamyl transpeptidase; LC-MS/MS, liquid chromatography–tandem mass spectrometry; LLOQ, lower than the limit of quantification; MRM, multiplexed multiple reaction monitoring; MDR, multidrug resistance protein; MRP, multidrug resistance-associated protein; OAT, organic anion transporter; OATP, organic anion transporting polypeptide; OCT, organic cation transporter; PXB mice, chimeric mice with humanized liver; P450R, NADPH-cytochrome P450 reductase; UGT, UDP-glucuronosyltransferases; uPA/SCID, urokinase-type plasminogen activator/severe combined immunodeficiency.

CYP3A4) and transporters in human livers; for example, the correlation coefficients (r^2) were less than 0.3 for CYP1A2, 2C9, 2A6, 2E1, UGT1A1, CYP2B7, multidrug resistance-associated protein 2 (MRP2), multidrug resistance protein 1 (MDR1), bile salt export pump (BSEP), multidrug and toxin extrusion protein 1 (MATE1), organic cation transporter (OCT1), sodium/taurocholate cotransporting polypeptide (NTCP), and organic anion transporting polypeptide (OATP)1B3 (Ohtsuki et al., 2012). Furthermore, metabolizing activities of P450s such as CYP2C9, 2C19, 2D6, and 2E1 were correlated to expression levels of protein rather than mRNA (Ohtsuki et al., 2012). In addition, human hepatocytes are transplanted to produce the PXB mice, so it is also important to consider the influence of the donor on the protein expression of metabolizing enzymes and transporters.

We have recently developed a liquid chromatography–tandem mass spectrometry (LC-MS/MS)–based protein quantification method that does not require antibodies (Kamiie et al., 2008). In this method, the target protein concentration in a sample is determined after enzymatic digestion by quantifying one or more peptide fragments specific to the target molecule. By using this method, we have measured protein expression levels of metabolizing enzymes and transporters in human and mouse livers (Kamiie et al., 2008; Kawakami et al., 2011; Ohtsuki et al., 2012). Since the target peptide is identified by mass-weight information, a single amino acid difference can be distinguished. Furthermore, the specificity, accuracy, and dynamic range of quantification by LC-MS/MS–based analysis [coefficient of variance (CV) < 20% and three-orders-of-magnitude dynamic range] are greatly superior to those in the case of immunoblot analysis (Kamiie et al., 2008; Kawakami et al., 2011; Ohtsuki et al., 2011). Therefore, this method was considered suitable for validating PXB mouse as a human liver model in terms of protein levels in the liver.

The purpose of the present study was to clarify the protein expression levels of metabolizing enzymes and transporters in liver of PXB mice transplanted with human hepatocytes from different donors by using LC-MS/MS, and to compare the protein expression levels with those of human livers to validate PXB mouse as a model of human liver.

Materials and Methods

Generation of PXB Mice. The present study was approved by the Ethics Committees of the Graduate School of Pharmaceutical Sciences, Tohoku University, and PhoenixBio Co., Ltd. The experiments in this report conformed to the guidelines established by the Animal Care Committee, Graduate School of Pharmaceutical Sciences, Tohoku University, and PhoenixBio Co., Ltd. The cryopreserved human hepatocytes from donor BD85 (black, male, 5 years old), BD72 (white, female, 10 years old), and BD87 (white, male, 2 years old) were purchased from BD BioSciences (San Jose, CA) (Supplemental Table 1). The chimeric mice with humanized liver were generated by the method described previously (Tateno et al., 2004). Briefly, uPA$^{+/+}$/SCID mice were prepared (Tateno et al., 2004), and at 3 weeks after birth they were injected with human hepatocytes through a small left-flank incision into the inferior splenic pole. The concentration of human albumin in the blood of the chimeric mice and the replacement index (RI; the rate of the replacement from mouse to human hepatocytes) were measured using latex agglutination immunonephelometry (LX Reagent "Eiken" Alb II; Eiken Chemical, Tokyo, Japan) and anti-human specific cytokeratin 8 and 18 antibody (Cappel Laboratory, Cochranville, PA), respectively (Supplemental Table 1). There was a good correlation between the human albumin concentration and the RI (Tateno et al., 2004). In this study, the chimeric mice used were 13–14 weeks of age.

LC-MS/MS–Based Protein Quantification Analysis. Microsomal and plasma membrane fractions of liver were prepared as described previously (Ohtsuki et al., 2012). For details, see Supplemental Data. Protein quantitation of the target molecules was simultaneously performed by means of high-performance (HP)LC-MS/MS for metabolizing enzymes or nanoLC-MS/MS for transporters with multiplexed multiple reaction monitoring (multiplexed

MRM) as described previously (Ohtsuki et al., 2011; Shawahna et al., 2011; Uchida et al., 2011). Protein expression levels were determined by quantifying specific target peptides produced by trypsin digestion (Supplemental Table 2). Absolute amounts of each target peptide were determined by using an internal standard peptide, which is a stable isotope-labeled peptide with an amino acid sequence identical to that of the corresponding target peptide. Details of the quantification procedure are given in Supplemental Data.

One specific peptide was selected for quantification of each target protein and measured at four different MRM transitions. The amount of each peptide was determined as an average of three or four MRM transitions from one sample. In cases where signal peaks of fewer than three transitions were obtained, the amount of peptide in the sample was defined as under the limit of quantification. The absolute expression amount of CYP3A4 was calculated from the quantitative data obtained for a peptide generated from both CYP3A4 and CYP3A43 by subtracting the value obtained for a peptide that is specific for CYP3A43. Since CYP3A43 was under the limit of quantification in all samples, quantification values obtained with CYP3A4/43 peptides were used as those of CYP3A4.

For the comparison of protein expression levels between humanized liver of PXB mice and human liver, the data for microsomal fraction of 17 human liver biopsies were taken from our previous publication (Ohtsuki et al., 2012).

Statistical Analysis. Statistical significance of differences among donors was determined by one-way analysis of variance followed by the Bonferroni test using Origin 9 software (OriginLab Corp., Northampton, MA).

Results

Protein Expression Levels of Metabolizing Enzymes in Microsomal Fraction of PXB Mouse Liver. Protein expression levels of 12 human P450 enzymes, human NADPH-cytochrome P450 reductase (P450R), Na$^+$/K$^+$ ATPase, and γ-glutamyl transpeptidase (γ-GTP) were determined in liver microsomal fraction of PXB mice with transplanted hepatocytes from three different donors (Table 1). Two human UGT enzymes were determined in hepatocytes from two different donors. Na$^+$/K$^+$ ATPase and γ-GTP are membrane markers, and both the human and mouse molecules were quantified. The coefficients of variance of their quantification values were 14.5% and 14.1%, respectively, among 11 samples, and the values were not significantly different among the three donors. This suggests that the purity of the microsomal fraction was similar in all cases.

CYP2E1, P450R, and UGT2B7 were expressed most abundantly at 51.8, 31.6, and 55.0 pmol/mg protein of microsomal fraction, respectively (Table 1). The highest CV among samples was 76.1% for CYP2A6. The average of %CV of all samples was 43.4%. This is significantly greater than those of the individual donors ($P < 0.05$), which were 26.5%, 23.9%, and 23.0% for BD85, BD72, and BD87, respectively, suggesting that differences among the donors contribute substantially to the variances of expression levels of the target proteins in all samples. CYP2C9, 2C8, 2A6, 2C19, 2D6, 2B6, and P450R showed significant differences in protein expression levels among donors ($P < 0.05$). In addition, CYP3A5 and 3A7 were determined in all five samples from donor BD85, but were not detected or were detected in only 1 sample from the other donors. CYP2D6 was detected in only one sample from donor BD72, but was detected in all samples from BD85 and BD87.

Protein Expression Levels of Transporters in Plasma Membrane Fraction of PXB Mouse Liver. Protein expression levels of seven human ABC transporters, eight human solute carrier transporters, Na$^+$/K$^+$ ATPase, and γ-GTP were determined in plasma membrane fraction of PXB mouse liver, since these drug transporters function at the plasma membrane (Table 2). Na$^+$/K$^+$ ATPase and γ-GTP are membrane markers, and the CVs of their quantification values were 29.4% and 40.1%, respectively, among 11 samples. The quantified values were not significantly different among the three

TABLE 1

Protein expression levels of metabolizing enzymes in microsomal fraction of humanized liver of PXB mice

Unit of protein expression is pmol/mg protein of microsomal fraction.

Donor	ALL (n =11)				BD85 (n = 5)				BD72 (n = 3)				BD87 (n = 3)			
	Mean	S.D.	%CV	n	Mean	S.D.	% CV	n	Mean	S.D.	%CV	n	Mean	S.D.	%CV	n
CYP2E1	51.8	9.7	18.7	11	51.7	9.4	18	5	52.9	7.8	15	3	50.9	15.2	30	3
CYP3A4	27.8	12.4	44.5	11	26.7	11.1	41	5	24.8	10.7	43	3	32.4	18.9	58	3
CYP2C9*	21.7	14.2	65.5	11	9.71	1.00	10	5	28.6	10.6	37	3	34.8	14.4	41	3
CYP1A2	20.7	6.4	30.9	11	23.3	5.1	22	5	16.5	7.1	43	3	20.4	7.7	38	3
CYP2C8*	15.8	6.3	39.8	11	10.2	1.8	18	5	16.9	1.9	11	3	24.1	2.1	9	3
CYP2A6*	10.2	7.8	76.1	11	2.93	0.40	14	5	12.4	1.6	13	3	20.2	3.3	16	3
CYP2C19*	8.84	6.25	70.8	11	4.90	1.15	24	5	16.6	7.2	43	3	7.59	2.99	39	3
CYP2D6*	7.07	2.94	41.6	11	6.77	1.64	24	5	1.23			1	9.51	1.75	18	3
CYP3A7	6.32	3.31	52.3	5	6.32	3.31	52	5	LLOQ				LLOQ			
CYP3A5	5.56	4.09	73.5	6	6.56	3.66	56	5	LLOQ				0.579			1
CYP4A11	5.04	1.97	39.1	9	4.85	1.99	41	5	2.29			1	6.26	1.24	20	3
CYP2B6*	1.90	0.91	47.6	11	1.68	0.49	30	5	1.08	0.27	25	3	3.11	0.45	15	3
P450R*	31.6	18.7	59.3	11	12.4	1.7	14	5	43.7	4.6	11	3	51.2	1.7	3	3
UGT2B7	55.0	20.8	37.8	6	N.D.				43.0	11.4	26	3	67.0	22.7	34	3
UGT1A1	19.0	2.4	12.5	6	N.D.				19.7	3.5	18	3	18.4	0.5	3	3
Na$^+$/K$^+$ ATPase	10.4	1.5	14.5	11	9.94	2.14	22	5	10.5	0.4	4	3	11.1	0.9	8	3
γ-GTP	2.64	0.37	14.1	11	2.57	0.33	13	5	2.64	0.55	21	3	2.74	0.37	13	3

n, Number of determined samples; LLOQ, lower than the limit of quantification; N.D., not determined.
*Significant difference (P < 0.05) in protein expression levels among donors (BD85, BD72, and BD87).

donors. This suggests that the purity of plasma membrane fraction was similar among donors, although the variability appeared to be greater than that of the microsomal fraction

All human transporters, except breast cancer resistance protein (BCRP), were quantified in all 11 samples (Table 2). MDR3 and BSEP exhibited the highest expression levels among the quantified transporters at 8.68 and 7.57 pmol/mg plasma membrane protein, respectively. Human BCRP was not detected in five samples from donor BD85, and was not quantified in samples from BD72 and BD87, in accordance with a report that BCRP expression is very low in human liver plasma membrane fraction (Ohtsuki et al., 2012). The average value of %CV of all samples was 47.0%, which was similar to

that of microsomal fraction (43.4%), and significantly greater than that of BD72 (25.5%, P < 0.01) or BD87 (25.6%, P < 0.01). It was also greater, though not significantly, than that of BD85 (35.4%). Therefore, differences among the donors appear to contribute substantially to the variances of protein expression levels in all samples. MDR3, BSEP, MRP2, ABCG8, OCT1, and OATP1B3 showed significantly different protein expression levels depending on the hepatocyte donors (P < 0.05).

Comparison of Protein Expression Levels in Liver of PXB Mice and Human. The protein expression levels of metabolizing enzymes and transporters in PXB mouse liver shown in Tables 1 and 2 were compared with those in human liver. The protein expression levels

TABLE 2

Protein expression levels of transporters in plasma membrane fraction of humanized liver of PXB mice

Unit of protein expression is pmol/mg protein of plasma membrane fraction.

Donor	ALL (n = 11)				BD85 (n = 5)				BD72 (n = 3)				BD87 (n = 3)			
	Mean	S.D.	%CV	n	Mean	S.D.	%CV	n	Mean	S.D.	%CV	n	Mean	S.D.	%CV	n
Canalicular localized transporter																
MDR3/ABCB4*	8.68	7.32	84.3	11	4.19	1.29	31	5	7.47	3.66	49	3	17.4	9.24	53	3
BSEP/ABCB11*	7.57	7.91	104	11	3.06	1.13	37	5	6.12	2.79	46	3	16.5	11.29	68	3
MDR1/ABCB1	4.71	1.78	37.7	11	4.30	1.55	36	5	3.86	1.19	31	3	6.26	2.10	34	3
MRP2/ABCC2*	2.37	0.88	37.1	11	2.06	0.91	44	5	1.89	0.19	10	3	3.36	0.34	10	3
MATE1	1.10	0.22	19.7	11	1.07	0.23	22	5	1.28	0.21	17	3	0.981	0.086	9	3
ABCG8*	0.956	0.701	73.3	11	0.417	0.106	25	5	1.89	0.62	33	3	0.921	0.132	14	3
BCRP/ABCG2	LLOQ				LLOQ				N.D.				N.D.			
γ-GTP	2.22	0.89	40.1	11	2.52	0.60	24	5	1.57	0.18	12	3	2.39	1.52	64	3
Sinusoidal localized transporter																
OCT1*	4.21	3.41	81.0	11	6.87	3.04	44	5	3.22	1.61	50	3	0.765	0.102	13	3
OAT2	4.09	1.18	28.8	11	4.89	1.08	22	5	3.76	1.06	28	3	3.09	0.49	16	3
NTCP	2.42	0.81	33.5	11	2.12	1.12	53	5	2.61	0.34	13	3	2.71	0.47	17	3
MRP6	2.29	0.51	22.2	11	2.57	0.58	23	5	1.97	0.48	25	3	2.14	0.08	4	3
OATP1B1	1.45	0.56	38.9	11	1.22	0.63	52	5	1.50	0.16	11	3	1.78	0.68	38	3
OATP1B3*	1.03	0.47	45.9	11	0.616	0.207	34	5	1.47	0.47	32	3	1.28	0.06	5	3
OATP2B1	0.578	0.241	42.5	11	0.684	0.320	47	5	0.500	0.119	24	3	0.442	0.090	20	3
Na$^+$/K$^+$ ATPase	22.6	6.65	29.4	11	23.6	9.00	38	5	22.0	1.7	8	3	21.7	7.22	33	3
Localization unknown																
ENT1	1.55	0.50	32.6	11	1.79	0.60	34	5	1.59	0.32	20	3	1.11	0.13	11	3

n, Number of determined samples; LLOQ, lower than the limit of quantification; N.D., not determined; ENT, equilibrative nucleoside transporter; NTCP, sodium/taurocholate cotransporting polypeptide.
*Significant difference (P < 0.05) in protein expression levels among donors (BD85, BD72 and BD87).

determined in 17 human liver biopsies (eight males and nine females, ages 20–74) were taken from our previous report (Ohtsuki et al., 2012). In the human liver biopsies, metabolizing enzymes and transporters were quantified in both microsomal fraction and plasma membrane fraction, as in the case of PXB mice. Expression levels of molecules determined both in PXB mouse and human livers are compared in Fig. 1. The differences between PXB mouse liver and human liver for all compared metabolizing enzymes and transporters were within 4-fold, except for CYP2A6 and CYP4A11 among metabolizing enzymes, and MDR3 and BSEP among transporters. Protein expression levels of CYP2A6 and CYP4A11 in PXB mouse liver microsomal fraction were 5.50- and 4.33-fold lower than those in human liver microsomal fraction, respectively. In contrast, protein expression levels of BSEP and MDR3 in PXB mouse liver plasma membrane fraction were 5.12- and 4.62-fold greater than those in human liver plasma membrane fraction.

Discussion

In the present study, we investigated the protein expression levels of human metabolizing enzymes in microsomal fraction and human membrane transporters in plasma membrane of humanized liver of PXB mice using LC-MS/MS–based protein quantification. In total, 11 livers of PXB mice humanized with hepatocytes from three different donors were quantified. Our results indicate that differences in the human donors contributed substantially to the variations of measured protein expression levels (Tables 1 and 2). This seems reasonable because the PXB mice were bred under controlled conditions, whereas the human donors might have been exposed to a variety of different environmental factors, such as food and drug intake, that could affect the expression of metabolizing enzymes and transporters.

Protein expression of CYP3A5 and CYP3A7 was detected in all liver samples from only one donor (BD85), and protein expression of CYP2D6 was detected in all liver samples from two donors (BD72 and BD87) (Table 1). In the previous study with PXB mice from two donors, CYP3A5 protein expression levels were very low in liver from both donors, and the reason for its low expression was genetic polymorphisms of the donor hepatocytes (Katoh et al., 2004). In our previous report, liver biopsies were clearly classified into two groups: a high-CYP3A7 group and a very low CYP3A7 group (Ohtsuki et al., 2012). Hence, the large differences in protein expression levels of these molecules might be attributable to differences in the genetic background of donor hepatocytes, although it is not known whether single-nucleotide polymorphisms were present in the transplanted human hepatocytes in our study. These results suggest that it is important to characterize the donor hepatocytes in studies with PXB mice; in principle, experiments should be performed with PXB mice humanized with hepatocytes from the same donor to ensure comparability of data.

In our previous reports, individual differences of BSEP protein expression were not large in plasma membrane fraction of human liver; the %CV was 29.7% among 17 liver biopsies (Ohtsuki et al., 2012). In contrast, %CV of BSEP protein expression was 105% in PXB liver (Table 2). A possible explanation is that BSEP expression is highly regulated in human liver, but lack of human-specific regulation in PXB mice resulted in a very high variance of protein expression. Interestingly, differences in MDR3 protein levels according to donor showed a trend similar to those of BSEP (Table 2). BSEP and MDR3 are cooperatively involved in excretion of lipids, and are regulated by FXR (Oude Elferink and Paulusma, 2007). Interspecies differences in FXR response have been reported (Cui et al., 2002; Song et al., 2013). Although further studies are necessary, it was possible that a shared

regulatory mechanism of BSEP and MDR3 played some role in the interdonor differences.

The present study demonstrated that protein expression levels of most of the quantified metabolizing enzymes and transporters were within a 4-fold range from those in the same fraction of human liver reported previously (Ohtsuki et al., 2012) (Fig. 1). This range of
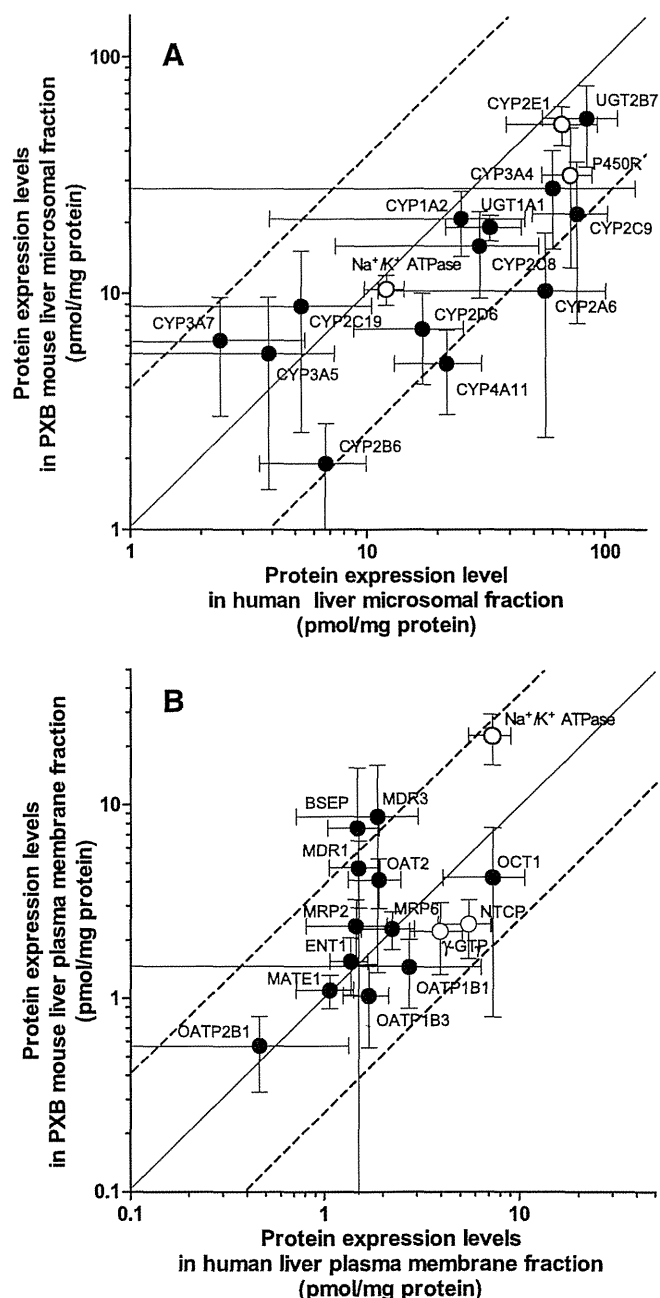

Fig. 1. Comparison of protein expression levels of metabolizing enzymes in microsomal fraction and transporters in plasma membrane fraction between humanized liver of PXB mice and human liver. Protein expression levels of metabolizing enzymes and transporters were determined in microsomal fraction (A) and plasma membrane fraction (B), respectively, of humanized liver of PXB mice, as shown in Tables 1 and 2 (mean ± S.D.). The data for microsomal fraction of 17 human liver biopsies (mean ± S.D.) were taken from our previous report (Ohtsuki et al., 2012). The solid line passing through the origin represents the line of identity, and the broken lines represent 4-fold differences. Open symbols indicate quantification values obtained with peptides that are conserved in the human and mouse proteins.

difference was the same as that in average expression levels among the three donors. The enzyme activities of P450 enzymes were reported to be better correlated to protein expression levels in the microsomal fraction than to mRNA expression levels (Ohtsuki et al., 2012). We compared the protein expression levels of transporters between PXB mice and human in plasma membrane fraction, where the quantified transporters function. A large species difference was reported in protein expression levels of BCRP in plasma membrane fraction: 0.419 pmol/mg protein in human liver and 8.51 pmol/mg protein in mouse liver (Kamiie et al., 2008; Ohtsuki et al., 2012). Here, human BCRP was under the limit of quantification in humanized liver of PXB mice, indicating that human hepatocytes retain the characteristic low expression of BCRP in PXB mice. Overall, our results indicate that humanized liver in PXB mice well retains the protein expression pattern of metabolizing enzymes and transporters of human liver.

Our previous report demonstrated that, in sandwich-cultured human hepatocytes, differences of protein expression levels of metabolizing enzymes and transporters compared with those in human liver were within a 5-fold range (Schaefer et al., 2012). A similar range of difference was found in liver of PXB mice in this study, though in cultured human hepatocytes, the protein expression levels of transporters tended to be greater than those in human liver. Since humanized liver retains the structure of human liver tissue (Tateno et al., 2013), our results suggest that humanized liver of PXB mice is a useful model for analyzing human hepatic drug metabolism in vivo.

In conclusion, we measured the protein expression levels of metabolizing enzymes in microsomal fraction and transporters in plasma membrane fraction of humanized liver of chimeric PXB mice. The protein expression levels of the quantified metabolizing enzymes and transporters well reflected those of the donor human liver. The protein expression in humanized liver was significantly affected by the background of each individual donor. Our results indicate that humanized liver of PXB mice is a useful model of human liver, but it is important to note that interpretation of the results obtained from PXB mice requires a knowledge of not only the value of the replacement index, but also information about the background of the hepatocyte donor.

Department of Pharmaceutical
Microbiology, Faculty of Life
Sciences, Kumamoto University,
Kumamoto, Japan (S.O., K.N.);
Laboratory of Veterinary Pathology,
School of Veterinary Medicine,
Azabu University, Kanagawa, Japan
(H.K., J.K.); Division of Membrane
Transport and Drug Targeting,
Graduate School of Pharmaceutical
Sciences, Tohoku University, Sendai,
Japan (T.I., Y.K., W.O., Y.U., T.T.);
PhoenixBio, Co., Ltd., Hiroshima,
Japan (C.T.); DeThree Research
Laboratory Inc., Ibaraki, Japan (T.H.)

SUMIO OHTSUKI
HIROTAKA KAWAKAMI
TAE INOUE
KENJI NAKAMURA
CHISE TATENO
YUKI KATSUKURA
WATARU OBUCHI
YASUO UCHIDA
JUNICHI KAMIIE
TORU HORIE
TETSUYA TERASAKI

Authorship Contributions

Participated in research design: Ohtsuki, Tateno, Kamiie, Horie, Terasaki.
Conducted experiments: Kawakami, Inoue, Nakamura, Katsukura.
Contributed new reagents or analytic tools: Obuchi, Uchida.
Performed data analysis: Ohtsuki, Kawakami, Inoue, Nakamura.

Wrote or contributed to the writing of the manuscript: Ohtsuki, Tateno, Horie, Terasaki.

References

Cui J, Heard TS, Yu J, Lo JL, Huang L, Li Y, Schaeffer JM, and Wright SD (2002) The amino acid residues asparagine 354 and isoleucine 372 of human farnesoid X receptor confer the receptor with high sensitivity to chenodeoxycholate. *J Biol Chem* 277:25963–25969.
De Serres M, Bowers G, Boyle G, Beaumont C, Castellino S, Sigafoos J, Dave M, Roberts A, Shah V, and Olson K, et al. (2011) Evaluation of a chimeric (uPA+/+)/SCID mouse model with a humanized liver for prediction of human metabolism. *Xenobiotica* 41:464–475.
Hasegawa M, Tahara H, Inoue R, Kakuni M, Tateno C, and Ushiki J (2012) Investigation of drug-drug interactions caused by human pregnane X receptor-mediated induction of CYP3A4 and CYP2C subfamilies in chimeric mice with a humanized liver. *Drug Metab Dispos* 40:474–480.
Inoue T, Sugihara K, Ohshita H, Horie T, Kitamura S, and Ohta S (2009) Prediction of human disposition toward S-3H-warfarin using chimeric mice with humanized liver. *Drug Metab Pharmacokinet* 24:153–160.
Kamiie J, Ohtsuki S, Iwase R, Ohmine K, Katsukura Y, Yanai K, Sekine Y, Uchida Y, Ito S, and Terasaki T (2008) Quantitative atlas of membrane transporter proteins: development and application of a highly sensitive simultaneous LC/MS/MS method combined with novel in-silico peptide selection criteria. *Pharm Res* 25:1469–1483.
Kamimura H, Nakada N, Suzuki K, Mera A, Souda K, Murakami Y, Tanaka K, Iwatsubo T, Kawamura A, and Usui T (2010) Assessment of chimeric mice with humanized liver as a tool for predicting circulating human metabolites. *Drug Metab Pharmacokinet* 25:223–235.
Katoh M, Matsui T, Nakajima M, Tateno C, Kataoka M, Soeno Y, Horie T, Iwasaki K, Yoshizato K, and Yokoi T (2004) Expression of human cytochromes P450 in chimeric mice with humanized liver. *Drug Metab Dispos* 32:1402–1410.
Katoh M, Matsui T, Okumura H, Nakajima M, Nishimura M, Naito S, Tateno C, Yoshizato K, and Yokoi T (2005) Expression of human phase II enzymes in chimeric mice with humanized liver. *Drug Metab Dispos* 33:1333–1340.
Kawakami H, Ohtsuki S, Kamiie J, Suzuki T, Abe T, and Terasaki T (2011) Simultaneous absolute quantification of 11 cytochrome P450 isoforms in human liver microsomes by liquid chromatography tandem mass spectrometry with in silico target peptide selection. *J Pharm Sci* 100:341–352.
Kikuchi R, McCown M, Olson P, Tateno C, Morikawa Y, Katoh Y, Bourdet DL, Monshouwer M, and Fretland AJ (2010) Effect of hepatitis C virus infection on the mRNA expression of drug transporters and cytochrome p450 enzymes in chimeric mice with humanized liver. *Drug Metab Dispos* 38:1954–1961.
Nishimura M, Yoshitsugu H, Yokoi T, Tateno C, Kataoka M, Horie T, Yoshizato K, and Naito S (2005) Evaluation of mRNA expression of human drug-metabolizing enzymes and transporters in chimeric mouse with humanized liver. *Xenobiotica* 35:877–890.
Ohtsuki S, Uchida Y, Kubo Y, and Terasaki T (2011) Quantitative targeted absolute proteomics-based ADME research as a new path to drug discovery and development: methodology, advantages, strategy, and prospects. *J Pharm Sci* 100:3547–3559.
Ohtsuki S, Schaefer O, Kawakami H, Inoue T, Liehner S, Saito A, Ishiguro N, Kishimoto W, Ludwig-Schwellinger E, and Ebner T, et al. (2012) Simultaneous absolute protein quantification of transporters, cytochromes P450, and UDP-glucuronosyltransferases as a novel approach for the characterization of individual human liver: comparison with mRNA levels and activities. *Drug Metab Dispos* 40:83–92.
Oude Elferink RP and Paulusma CC (2007) Function and pathophysiological importance of ABCB4 (MDR3 P-glycoprotein). *Pflugers Arch* 453:601–610.
Schaefer O, Ohtsuki S, Kawakami H, Inoue T, Liehner S, Saito A, Sakamoto A, Ishiguro N, Matsumaru T, and Terasaki T, et al. (2012) Absolute quantification and differential expression of drug transporters, cytochrome P450 enzymes, and UDP-glucuronosyltransferases in cultured primary human hepatocytes. *Drug Metab Dispos* 40:93–103.
Shawahna R, Uchida Y, Declèves X, Yousif S, Dauchy S, Jacob A, Chassoux F, Daumas-Duport C, and Couraud PO, et al. (2011) Transcriptomic and quantitative proteomic analysis of transporters and drug metabolizing enzymes in freshly isolated human brain microvessels. *Mol Pharm* 8:1332–1341.
Song X, Chen Y, Valanejad L, Kaimal R, Yan B, Stoner M, and Deng R (2013) Mechanistic insights into isoform-dependent and species-specific regulation of bile salt export pump by farnesoid X receptor. *J Lipid Res* 54:3030–3044.
Tateno C, Yoshizane Y, Saito N, Kataoka M, Utoh R, Yamasaki C, Tachibana A, Soeno Y, Asahina K, and Hino H, et al. (2004) Near completely humanized liver in mice shows human-type metabolic responses to drugs. *Am J Pathol* 165:901–912.
Tateno C, Miya F, Wake K, Kataoka M, Ishida Y, Yamasaki C, Yanagi A, Kakuni M, Wisse E, and Verheyen F, et al. (2013) Morphological and microarray analyses of human hepatocytes from xenogeneic host livers. *Lab Invest* 93:54–71.
Uchida Y, Ohtsuki S, Katsukura Y, Ikeda C, Suzuki T, Kamiie J, and Terasaki T (2011) Quantitative targeted absolute proteomics of human blood-brain barrier transporters and receptors. *J Neurochem* 117:333–345.
Yamazaki H, Kuribayashi S, Inoue T, Tateno C, Nishikura Y, Oofusa K, Harada D, Naito S, Horie T, and Ohta S (2010) Approach for in vivo protein binding of 5-n-butyl-pyrazolo[1,5-a] pyrimidine bioactivated in chimeric mice with humanized liver by two-dimensional electrophoresis with accelerator mass spectrometry. *Chem Res Toxicol* 23:152–158.

Address correspondence to: Dr. Tetsuya Terasaki, Division of Membrane Transport and Drug Targeting Laboratory, Department of Biochemical Pharmacology and Therapeutics, Graduate School of Pharmaceutical Sciences, Tohoku University, 6-3 Aoba, Aramaki, Aoba-ku Sendai 980-8578, Japan. E-mail: terasaki.tetsuya@m.tohoku.ac.jp

Impaired Interferon Signaling in Chronic Hepatitis C Patients With Advanced Fibrosis via the Transforming Growth Factor Beta Signaling Pathway

Takayoshi Shirasaki,[1,2] Masao Honda,[1,2] Tetsuro Shimakami,[1] Kazuhisa Murai,[1,2] Takayuki Shiomoto,[1,2] Hikari Okada,[1] Riuta Takabatake,[1] Akihiro Tokumaru,[1] Yoshio Sakai,[1] Taro Yamashita,[1] Stanley M. Lemon,[3] Seishi Murakami,[1] and Shuichi Kaneko[1]

Malnutrition in the advanced fibrosis stage of chronic hepatitis C (CH-C) impairs interferon (IFN) signaling by inhibiting mammalian target of rapamycin complex 1 (mTORC1) signaling. However, the effect of profibrotic signaling on IFN signaling is not known. Here, the effect of transforming growth factor (TGF)-β signaling on IFN signaling and hepatitis C virus (HCV) replication was examined in Huh-7.5 cells by evaluating the expression of forkhead box O3A (Foxo3a), suppressor of cytokine signaling 3 (Socs3), c-Jun, activating transcription factor 2, ras homolog enriched in brain, and mTORC1. The findings were confirmed in liver tissue samples obtained from 91 patients who received pegylated-IFN and ribavirin combination therapy. TGF-β signaling was significantly up-regulated in the advanced fibrosis stage of CH-C. A significant positive correlation was observed between the expression of TGF-β2 and mothers against decapentaplegic homolog 2 (Smad2), Smad2 and Foxo3a, and Foxo3a and Socs3 in the liver of CH-C patients. In Huh-7.5 cells, TGF-β1 activated the Foxo3a promoter through an AP1 binding site; the transcription factor c-Jun was involved in this activation. Foxo3a activated the Socs3 promoter and increased HCV replication. TGF-β1 also inhibited mTORC1 and IFN signaling. Interestingly, c-Jun and TGF-β signaling was up-regulated in treatment-resistant IL28B minor genotype patients (TG/GG at rs8099917), especially in the early fibrosis stage. Branched chain amino acids or a TGF-β receptor inhibitor canceled these effects and showed an additive effect on the anti-HCV activity of direct-acting antiviral drugs (DAAs). *Conclusion:* Blocking TGF-β signaling could potentiate the antiviral efficacy of IFN- and/ or DAA-based treatment regimens and would be useful for the treatment of difficult-to-cure CH-C patients. (HEPATOLOGY 2014;60:1519-1530)

A human liver infected with hepatitis C virus (HCV) develops chronic hepatitis, cirrhosis, and in some instances, hepatocellular carcinoma (HCC). HCC develops frequently in the advanced fibrosis stage, and the annual incidence of HCC in patients with HCV-related liver cirrhosis is ~6-8%.[1] The eradication of HCV infection has been a promising prophylactic therapy for preventing the occurrence of HCC.

Interferon (IFN) and ribavirin (RBV) combination therapy has been a popular modality for eliminating HCV; however, its efficacy is limited in patients with advanced liver fibrosis.[2] The use of the recently developed direct-acting antiviral drugs (DAAs) telaprevir or

1519

boceprevir, combined with pegylated (PEG)-IFN plus RBV, significantly improved the sustained virologic response (SVR) rates; however, the SVR rate is reduced in patients with advanced liver fibrosis and the treatment-resistant interleukin 28B (IL28B) genotype,[3-5] in whom HCC can develop at a high frequency. Moreover, extended therapy should be avoided in these patients in terms of the high frequency of adverse effects.

The mechanism of treatment resistance in patients with advanced liver fibrosis has not yet been clarified completely. Previously, we reported that the malnutrition status of patients with advanced chronic hepatitis C (CH-C) is associated with IFN resistance, and Fischer's ratio (branched chain amino acids [BCAAs] / aromatic amino acids) is an independent predictor of treatment outcome of PEG-IFN plus RBV combination therapy. Furthermore, we showed that malnutrition impaired IFN signaling by inhibiting mammalian target of rapamycin complex 1 (mTORC1) and activating suppressor of cytokine signaling 3 (Socs3)-mediated IFN inhibitory signaling through the nutrition-sensing transcriptional factor forkhead box protein O3a (Foxo3a).[6] This report represented the first clue to disentangling the molecular links between advanced CH-C and poor treatment response; however, the association of profibrotic signaling and IFN signaling was not evaluated in detail.

In the present study, we investigated the interaction between the signaling of the profibrotic gene transforming growth factor (TGF)-β and IFN signaling in the liver of CH-C patients. We showed that blocking TGF-β signaling as well as improving the nutritional status of patients by using BCAAs restored IFN signaling and increased the treatment efficacy of anti-HCV therapy.

Materials and Methods

Cell Lines. A reversibly immortalized human hepatocyte cell line (TTNT) was established by transduction with a retroviral vector containing cDNA expressing hTERT for immortalization.[7] TTNT, Huh-7, and Huh-7.5 cells (kindly provided by Professor C.M. Rice, Rockefeller University, New York, NY)

were maintained in Dulbecco's modified Eagle's medium (DMEM; Gibco BRL, Gaithersburg, MD) containing 10% fetal bovine serum and 1% penicillin/streptomycin. Primary human hepatocytes (PHH) were isolated from chimeric mice with a humanized liver (PXB-mice; PhoenixBio, Hiroshima, Japan).

Amino Acid-Free Medium and BCAAs. Amino acid-free medium and BCAAs were prepared as described previously. Details are given in the Supporting Materials and Methods.

TGF-β and IFN Treatment. Huh-7.5 cells or HCV-RNA-transfected Huh-7.5 cells were seeded at 1.0×10^5 cells/well in 12-well plates. After 24 hours, the cells were treated with TGF-β (Millipore, Billerica, MA). At 24 hours later, the cells were treated with the indicated international units of IFN-α for 24 hours (Schering-Plough, Tokyo, Japan).

BCAA Treatment. HCV-RNA-transfected Huh-7.5 cells were seeded at 1.0×10^5 cells/well in 12-well plates. After 24 hours, the cells were treated with TGF-β in low-amino-acid medium and the indicated concentration of BCAAs. At 48 hours after treatment, real-time detection, polymerase chain reaction (RTD-PCR), western blotting, and *Gaussia* luciferase assays were carried out as described previously.

TGF-β Receptor Inhibitor Treatment. HCV-RNA-transfected Huh-7.5 cells were seeded at 1.0×10^5 cells/well in 12-well plates. After 24 hours, the cells were treated with TGF-β in low-amino-acid medium and TGF-β Receptor Inhibitor (TGF-β RI; Millipore). At 24 hours after treatment, RTD-PCR, western blotting, and *Gaussia* luciferase assays were carried out as described previously.

DAA Treatment. DAAs (boceprevir and BMS-790052) were purchased from AdooQ Bioscience (Irvine, CA). HCV-RNA-transfected Huh-7.5 cells were seeded at 1.0×10^5 cells/well in 12-well plates. After 24 hours, the cells were treated with TGF-β in low-amino-acid medium and BCAAs and DAAs. At 24 hours after treatment, the *Gaussia* luciferase assay was carried out as described previously.

Patients' characteristics, HCV replication analysis, western blotting, quantitative RTD-PCR, and promoter analysis are described in the Supporting Materials and Methods.
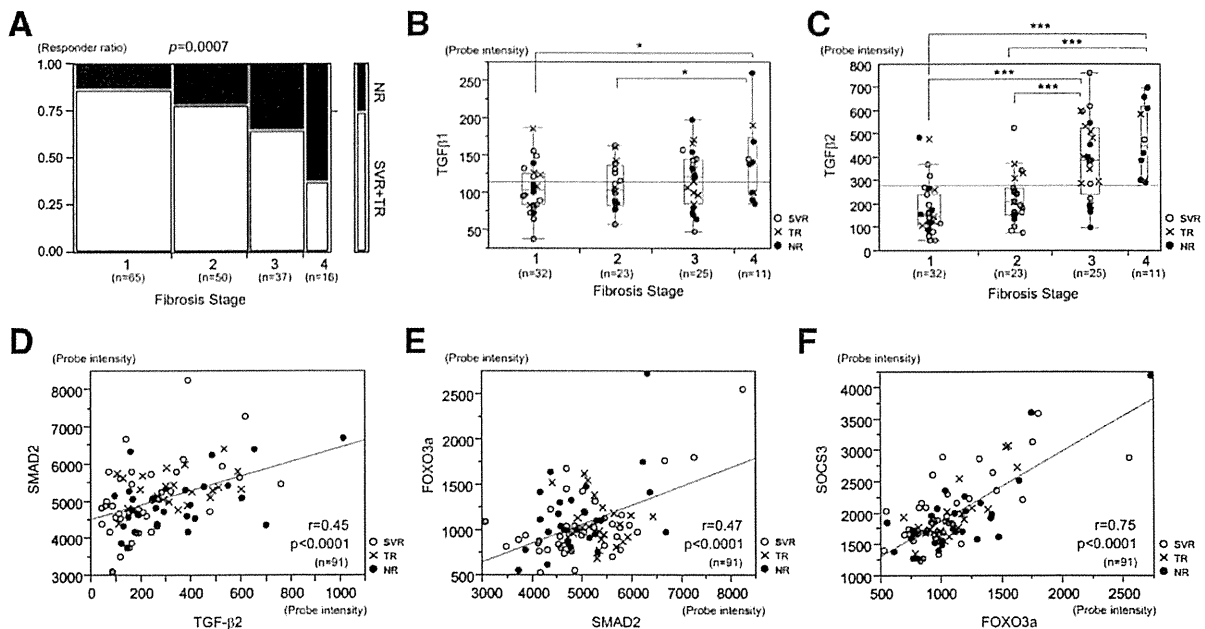
Fig. 1. Activation of TGF-β signaling in the liver of patients at the advanced fibrosis stage of CH-C. A: Significant increase in the NR ratio with the progression of fibrosis stage. B,C: Expression of TGF-β1 (B) and TGF-β2 (C) with the progression of fibrosis stage. D-F: Significant correlations of TGF-β2 and Smad2 (D), Smad2 and Foxo3a (E), and Foxo3a and Socs3 (F) expression in the liver of CH-C patients.

Statistical Analysis. The results are expressed as the mean value $\pm$ standard deviation. At least three samples were tested in each assay. Significance was tested by one-way analysis of variance with Bonferroni methods, and differences were considered statistically significant at $P < 0.05$.

Results

Up-Regulated TGF-β Signaling and Low Treatment Response in CH-C Patients With Advanced Liver Fibrosis Who Received PEG-IFN Plus RBV Combination Therapy. Previously, using a cohort of 168 CH-C patients who received PEG-IFN plus RBV combination therapy, we demonstrated that liver fibrosis stage and Fischer's ratio as well as IL28B genotype were independent significant factors associated with no response (NR) to treatment (Supporting Table 1).[6] The NR rate was significantly increased according to the increase in fibrosis stage ($P = 0.007$) (Fig. 1A). To reveal the molecular mechanism between profibrotic signaling and treatment resistance, we focused on TGF-β signaling in the liver of CH-C patients. The expression of TGF-β1 and TGF-β2, deduced from 91 CH-C patients whose liver tissues were analyzed previously using an Affymetrix GeneChip (Supporting Table 2),[6,8] was significantly up-regulated in the advanced fibrosis

stage (Fig. 1B,C). In particular, the up-regulation of TGF-β2 in patients with stage 3 and 4 fibrotic livers was more prominent (Fig. 1C). There was a significant correlation between the expression of TGF-β2 and mothers against decapentaplegic homolog 2 (Smad2), a downstream signaling molecule of the TGF-β receptor, showing the activation of TGF-β signaling in the liver of CH-C patients. Interestingly, Smad2 expression was significantly correlated with Foxo3a expression, a nutrition-sensing transcription factor. Previously, we reported that Foxo3a increases the transcription of Socs3, an inhibitor of IFN signaling, through binding to the Socs3 promoter (Foxo3a-Socs3 signaling).[6] Foxo3a expression was significantly correlated with Socs3 expression in the CH-C patients (Fig. 1F).

TGF-β Signaling Activates Foxo3a-Socs3 Signaling in the Huh-7.5 Human Hepatoma Cell Line and PHH. The relationship between TGF-β and Foxo3a-Socs3 signaling was evaluated in PHH and the Huh-7.5 human hepatoma cell line without HCV replication (Huh-7.5 HCV (–)). This signaling was also evaluated in Huh-7.5 cells in which the infectious HCV clone H77Sv3 GLuc2A[6] was replicating (Huh-7.5 HCV (+)) (Fig. 2A). Treatment of these cells with TGF-β1 substantially increased the levels of phosphorylated (p)-Smad2 and p-Smad3. In this condition, the levels of p-Foxo3a, which is degraded through the proteasomal pathway,
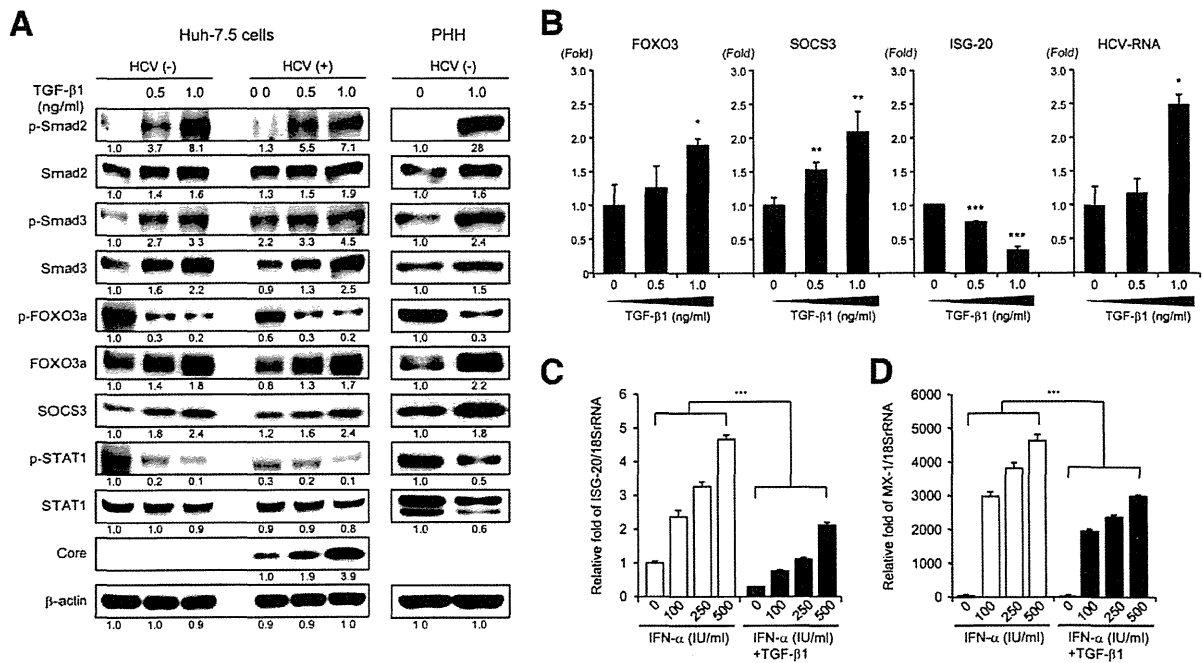
Fig. 2. Effect of TGF-β1 on IFN signaling in Huh-7.5 cells and PHH. A: Western blotting of TGF-β, Foxo3a-Socs3, and IFN signaling in Huh-7.5 cells and PHH treated with TGF-β1. Huh-7.5 cells were transfected with infectious HCV RNA, H77Sv3 GLuc2A prior to TGF-β1 treatment (Huh-7.5 HCV (+)). The experiments were repeated 3 times. B: RTD-PCR results for Foxo3a, Socs3, ISG-20, and HCV-RNA expression in Huh-7.5 HCV (+) treated with TGF-β1. C,D: Inhibition of IFN-α-induced ISG induction (ISG-20 [C] and MX1 [D]) by TGF-β1 in Huh-7.5 HCV (+). B-D: The experiments were performed in triplicate and repeated 3 times (*$P < 0.05$, **$P < 0.01$, ***$P < 0.001$).

decreased and total Foxo3a expression increased, and then Socs3 expression increased. Subsequently, the levels of phosphorylated signal transducer and activator of transcription 1 (p-STAT1) were decreased and the amount of HCV core protein increased in Huh-7.5 HCV (+). Thus, TGF-β signaling activated Foxo3a-Socs3 signaling and inhibited IFN signaling in hepatocytes, regardless of HCV replication and a loss-of-function mutation in retinoic acid inducible gene I (RIG-I).

These findings were also confirmed at the mRNA level in Huh-7.5 HCV (+). RTD-PCR showed that TGF-β1 treatment significantly increased Foxo3a and Socs3 expression, and decreased the expression of interferon-stimulated exonuclease gene 20 (ISG-20) in a dose-dependent manner. HCV-RNA was significantly increased in this condition (Fig. 2B). Moreover, the induction of interferon-stimulated genes (ISG-20 and myxovirus-resistance 1 [MX1]) by IFN-α treatment was significantly reduced in the presence of TGF-β1 (Fig. 2C,D).

When endogenous TGF-β signaling was compared between Huh-7.5 HCV (-) and Huh-7.5 HCV (+), TGF-β signaling was preactivated in Huh-7.5 HCV (+) before TGF-β1 treatment (Fig. 2A). To examine the role of endogenous TGF-β1 signaling on Foxo3a-Socs3 signaling and HCV replication, a small interfer-

ing (si) RNA specific to TGF-β1 was introduced to Huh-7 cells in which cell culture-derived infectious HCV HJ3-5 (HCVcc HJ3-5)[9] (Supporting Materials and Methods) was replicating. With the repression of TGF-β1, the levels of p-Smad2, p-Smad3, Foxo3a, and Socs3a decreased, while the levels of p-STAT1 increased. As a result, HCV replication deceased in both the amino acid-depleted (1/5 DMEM) and non-depleted (DMEM) conditions (Supporting Fig. 1).

AP1 Binding Site in the Foxo3a Promoter Is Responsible for the Induction of Foxo3a by TGF-β Signaling. To identify which transcription factors were involved in the induction of Foxo3a by TGF-β1, we cloned the upstream promoter region of Foxo3a and generated Foxo3a promoter-luciferase reporter constructs with various lengths of 5'-end deletions (−1780, −1340, and −801 nucleotides [nt]) (Fig. 3A). Luciferase activity deduced from pGL4-FOXO3a (−1780) increased by ∼1.5-fold in the amino acid-depleted condition (1/5 DMEM) compared with the nondepleted condition (DMEM). TGF-β1 further stimulated the promoter activity of pGL4-FOXO3a (−1780) (Fig. 3B). A TGF-β1 RI canceled this stimulation (Fig. 3B). pGL4-FOXO3a (−1340) retained the regulation of promoter activity by amino acid depletion (1/5 DMEM) and
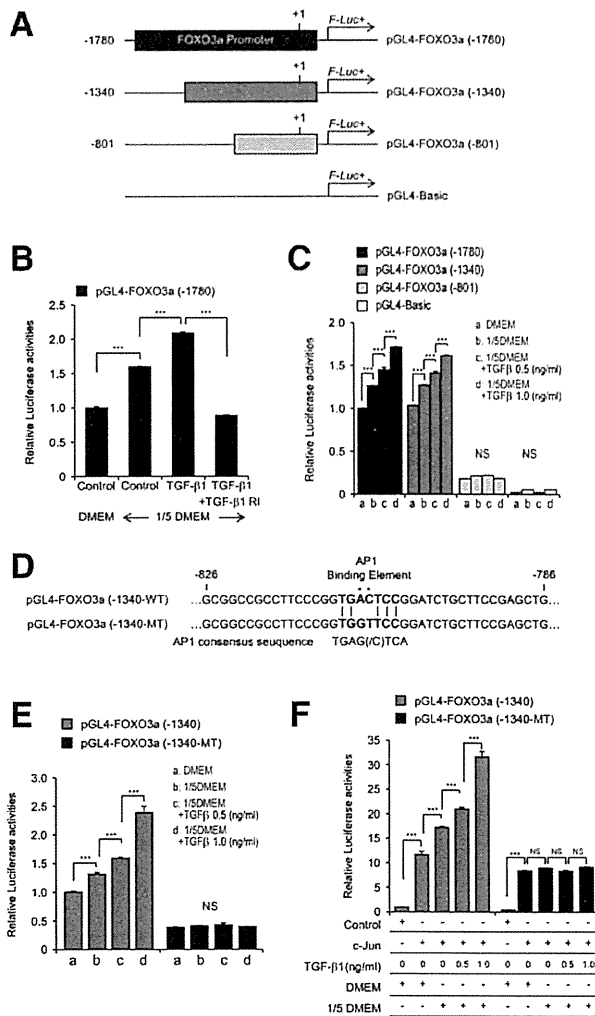
Fig. 3. Foxo3a promoter analysis. A: Foxo3a promoter-luciferase reporter constructs. B: Promoter activity of pGL4-FOXO3a (−1780) following amino acid depletion (1/5 DMEM), TGF-β1 treatment, and TGF-β1 RI treatment. C: Abolished regulation of the promoter activity of pGL4-FOXO3a (−801) by amino acid depletion (1/5 DMEM) and TGF-β1 treatment. D: Alignment of the AP1 binding element of pGL4-FOXO3a (−1340) and pGL4-FOXO3a (−1340-MT), in which the AP1 site was mutated. E: Abolished regulation of the promoter activity of pGL4-FOXO3a (−1340-MT) by amino acid depletion (1/5 DMEM) and TGF-β1 treatment. F: Overexpression of c-Jun, amino acid depletion (1/5 DMEM), and TGF-β1 treatment increased the promoter activity of pGL4-FOXO3a (−1340) by up to 32-fold, while these had less of an effect on the promoter activity of pGL4-FOXO3a (−1340-MT). The experiments were performed in triplicate and repeated 3 times ($*P < 0.05$, $**P < 0.01$, $***P < 0.001$).

TGF-β1 treatment; however, pGL4-FOXO3a (−801) lost this regulation (Fig. 3C), suggesting the presence of a response element between −1340 and −801 nt. We identified an activator protein (AP) 1 transcription factor binding site at −810 to −804 nt. (Fig. 3D). We introduced two nucleotide mutations (AC to GT) in the AP1 consensus binding sequence, and the mutant construct,

pGL4-FOXO3a (−1340-MT), lost the response to amino acid depletion (1/5 DMEM) and TGF-β1 treatment (Fig. 3E). These results were confirmed by using three different hepatocyte-derived cell lines (TTNT, Huh-7, and Huh-7.5 cells; Supporting Fig. 2A-C). Although RIG-I-dependent IFN signaling was active in TTNT cells (Supporting Fig. 2D), Foxo3a promoter activity in response to amino acid depletion (1/5 DMEM) and TGF-β1 treatment was not significantly different between these cell lines.

To confirm these findings further, we overexpressed c-Jun, a component of AP1, and evaluated Foxo3a promoter activity. The overexpression of c-Jun increased the promoter activity of pGL4-FOXO3a (−1340) to 12-fold, and amino acid depletion (1/5 DMEM) and TGF-β1 treatment further increased promoter activity up to 32-fold (Fig. 3F). Conversely, pGL4-FOXO3a (−1340-MT) lost the response to amino acid depletion (1/5 DMEM) and TGF-β1 treatment (Fig. 3F). These results confirmed that AP1 plays an important role in the induction of Foxo3a by these stimulatory factors.

Transcription Factor c-Jun Is Involved in the Induction of Foxo3a in the Liver of CH-C Patients. The AP1 transcription factor is mainly composed of Jun, Fos, and activating transcription factor (ATF) protein dimers.[10] Therefore, we evaluated the expression of c-Jun, ATF2, and c-Fos in Huh-7.5 cells and PHH under amino acid depletion (1/5 DMEM) and TGF-β1 treatment. Western blotting analysis showed that the levels of p-c-Jun and p-ATF2 were increased under these conditions, although the induction of p-c-Jun by amino acid depletion (1/5 DMEM) was not obvious in PHH (Fig. 4A). These findings were also confirmed by RTD-PCR. The mRNA expression of c-Jun and ATF2 increased significantly, while the expression of c-Fos decreased (Supporting Fig. 3A-C). The overexpression of c-Jun in Huh-7.5 cells induced Foxo3a and Socs3 expression at the protein and mRNA levels (Supporting Fig. 3D,E). In the liver of CH-C patients, there were significant correlations between the expression of Smad2 and c-Jun, and c-Jun and Foxo3a (Fig. 4B,C). ATF2 expression was significantly correlated with c-Jun expression (Fig. 4D). Similarly, there were significant correlations between the expression of Smad2 and ATF2, and ATF2 and Foxo3a (Fig. 4E,F). These results suggested that c-Jun and possibly ATF2, but not c-Fos, might be involved in TGF-β-Foxo3a signaling.

TGF-β Signaling Induces Socs3 Through the Induction of Foxo3a. Previously, we reported that Foxo3a increases the transcription of Socs3 through its binding to the Socs3 promoter region.[6] We confirmed
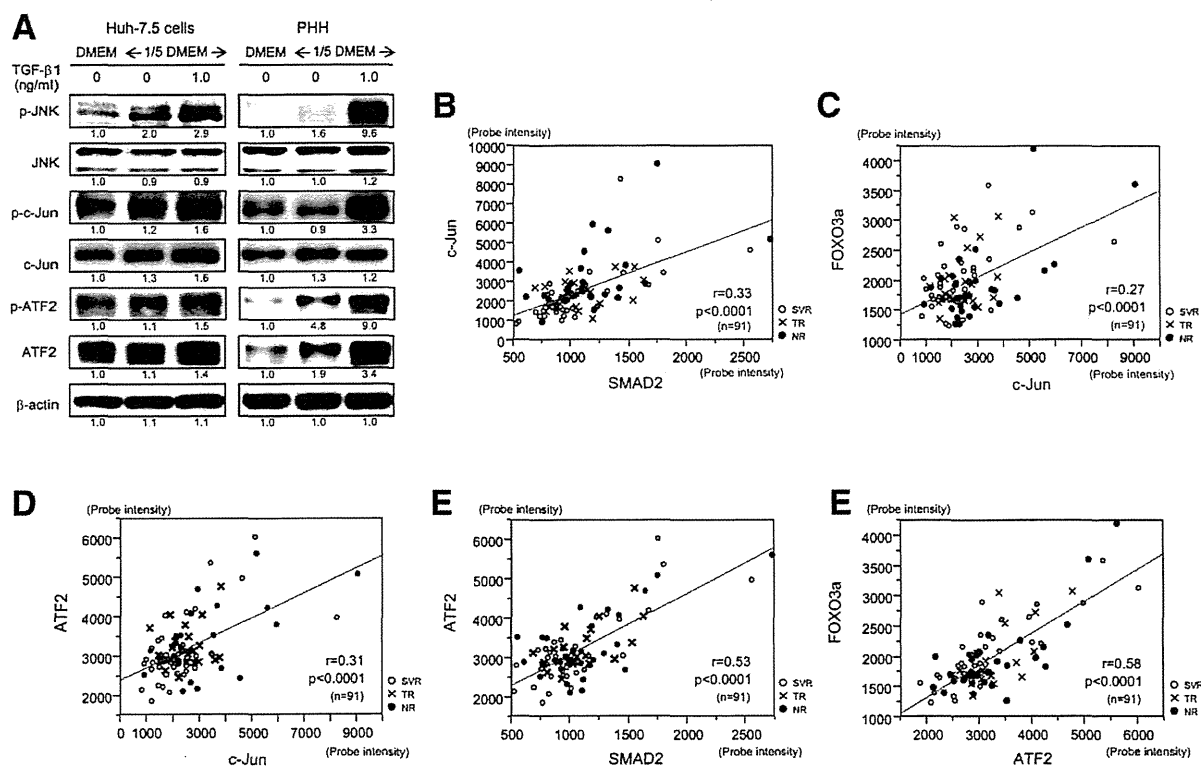
Fig. 4. TGF-β signaling up-regulates the expression of the transcription factors c-Jun and ATF2 in Huh-7.5 cells, PHH, and the liver of CH-C patients. A: Western blotting of JNK, c-Jun, and ATF2 in Huh-7.5 cells and PHH treated with amino acid depletion (1/5 DMEM) and TGF-β1. The experiments were repeated 3 times. B-F: Significant correlations of Smad2 and c-Jun (B), Foxo3a and c-Jun (C), c-Jun and ATF2 (D), Smad2 and ATF2 (E), and ATF2 and Foxo3a (F) expression in the liver of CH-C patients.

these findings in more detail in conjunction with TGF-β signaling. The overexpression of Foxo3a increased Socs3 expression in the nonamino acid-depleted condition (DMEM), and Socs3 was further induced in the amino acid-depleted condition (1/5 DMEM) and by TGF-β1 treatment (Supporting Fig. 4A). HCV-RNA was similarly increased in these conditions (Supporting Fig. 4B). Foxo3a mRNA expression, as deduced from RTD-PCR, was increased up to 7-fold in the combination of amino acid depletion (1/5 DMEM), c-Jun overexpression, and TGF-β1 treatment (Supporting Fig. 4C). Socs3 mRNA expression was up-regulated by 8-fold in the same conditions (Supporting Fig. 4D). The promoter activity of Socs3 was significantly increased by amino acid depletion (1/5 DMEM) and TGF-β1 treatment (pGL4-SOCS3-WT, Supporting Fig. 4E), while mutation of the Foxo3a binding site in the Socs3 promoter (pGL4-SOCS3-MT) abrogated this regulation. These results confirmed that TGF-β signaling up-regulated the expression of Socs3 through the induction of Foxo3a.

TGF-β Signaling Suppresses mTORC1 Signaling. Previously, we demonstrated that malnutrition decreased mTORC1 and IFN signaling using Huh-7 cells and clinical samples.[6] In the present study, we examined the effect of TGF-β signaling on mTORC1 signaling. In Huh-7.5 cells and PHH, amino acid depletion (1/5 DMEM) repressed mTORC1 signaling, as demonstrated by the decreased expression of ras homolog enriched in brain (RHEB),[11] a stimulator of mTORC1 signaling, p-mTOR, and p-p70S6K (Fig. 5A). Interestingly, TGF-β1 further decreased this expression. The decreased mTORC1 signaling was independent of AMP-activated, alpha 1 catalytic subunit (AMPK), a suppressor of mTORC1 signaling, as the levels of p-AMPK were rather decreased by amino acid depletion (1/5 DMEM) and TGF-β1 treatment in Huh-7.5 cells and PHH (Fig. 5A). It could be speculated that TGF-β signaling, combined with malnutrition, repressed the expression of RHEB and induced the expression of Foxo3a, which leads to the impaired IFN signaling observed in the advanced fibrosis stage of CH-C (Fig. 5B). In the liver of CH-C
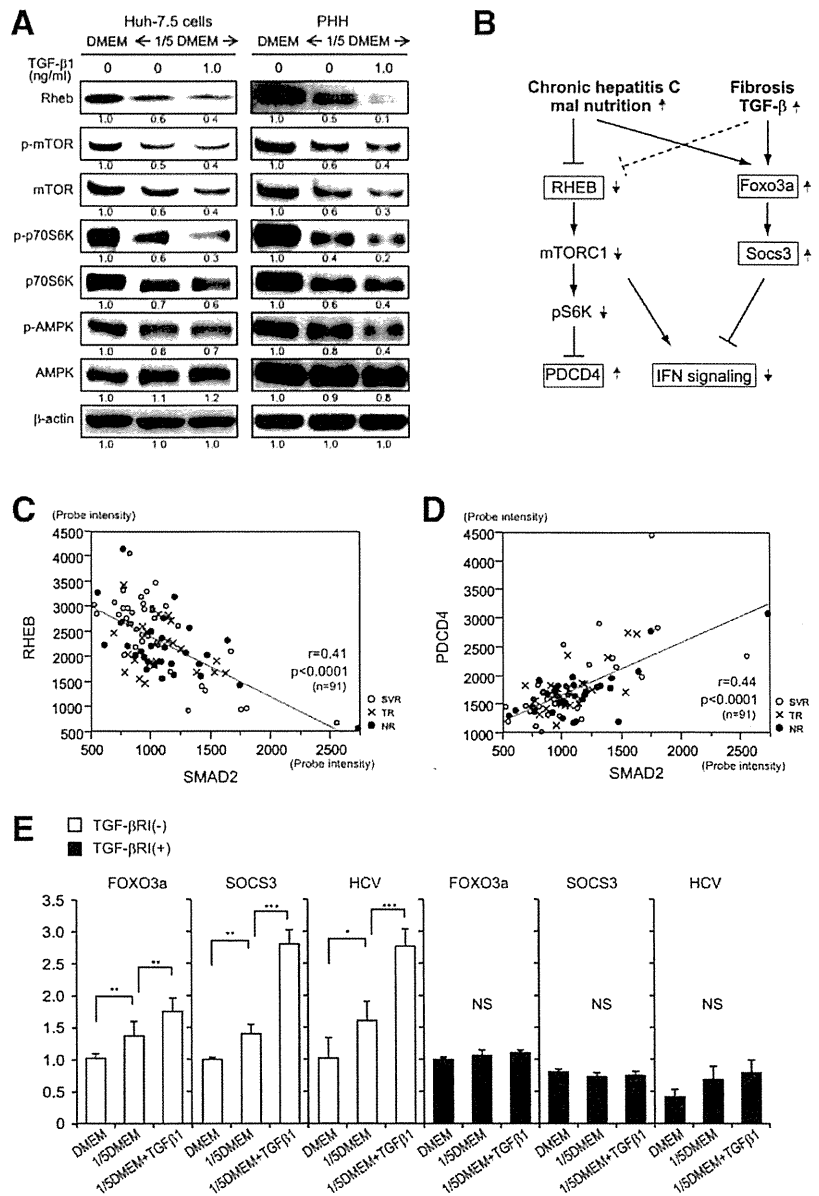
Fig. 5. TGF-β signaling represses mTORC1 signaling in Huh-7.5 cells, PHH, and the liver of CH-C patients. A: Western blotting of RHEB, mTOR, p70S8K, and AMPK in Huh-7.5 cells and PHH treated with amino acid depletion (1/5 DMEM) and TGF-β1. The experiments were repeated 3 times. B: Schematic representation of the effects of malnutrition and TGF-β signaling on IFN signaling. C,D: Significant correlations of Smad2 and RHEB (C), and Smad2 and PDCD4 (D) expression in the liver of CH-C patients. E: Blocking TGF-β signaling by TGF-β1 RI treatment abolishes the increase in Foxo3a, Socs3, and HCV replication by amino acid depletion (1/5 DMEM) and TGF-β1 treatment. The experiments were performed in triplicate and repeated 3 times ($*P < 0.05$, $**P < 0.01$, $***P < 0.001$).

patients, Smad2 expression was significantly negatively correlated with RHEB expression. The expression of programmed cell death 4 (PDCD4), which is negatively regulated by mTORC1 signaling at the transcriptional level (Fig. 5C),[12] was significantly positively correlated with Smad2 expression (Fig. 5D).

We further examined the effect of TGF-β1 on IFN signaling by using TGF-β RI. TGF-β RI substantially repressed the levels of p-Smad2 and p-Smad3 (Supporting Fig. 5). TGF-β RI abolished the induction of Foxo3a expression and the subsequent induction of Socs3 by amino acid depletion (1/5 DMEM) and TGF-β1 treatment (Fig. 5E). HCV replication in nor-

mal medium (DMEM), as deduced from *Gaussia* luciferase activity, was repressed by TGF-β RI, and the increase in HCV replication by amino acid depletion (1/5 DMEM) and TGF-β1 treatment was abrogated (Fig. 5E).

c-Jun Is Up-Regulated in the Liver of NR and Treatment-Resistant IL28B Minor Genotype Patients. We evaluated the clinical significance of c-Jun for treatment response. The expression of c-Jun was significantly higher in NR patients than in responder patients (SVR+TR) (Fig. 6A). Furthermore, c-Jun expression was significantly higher in patients with the treatment-resistant IL28B minor genotype
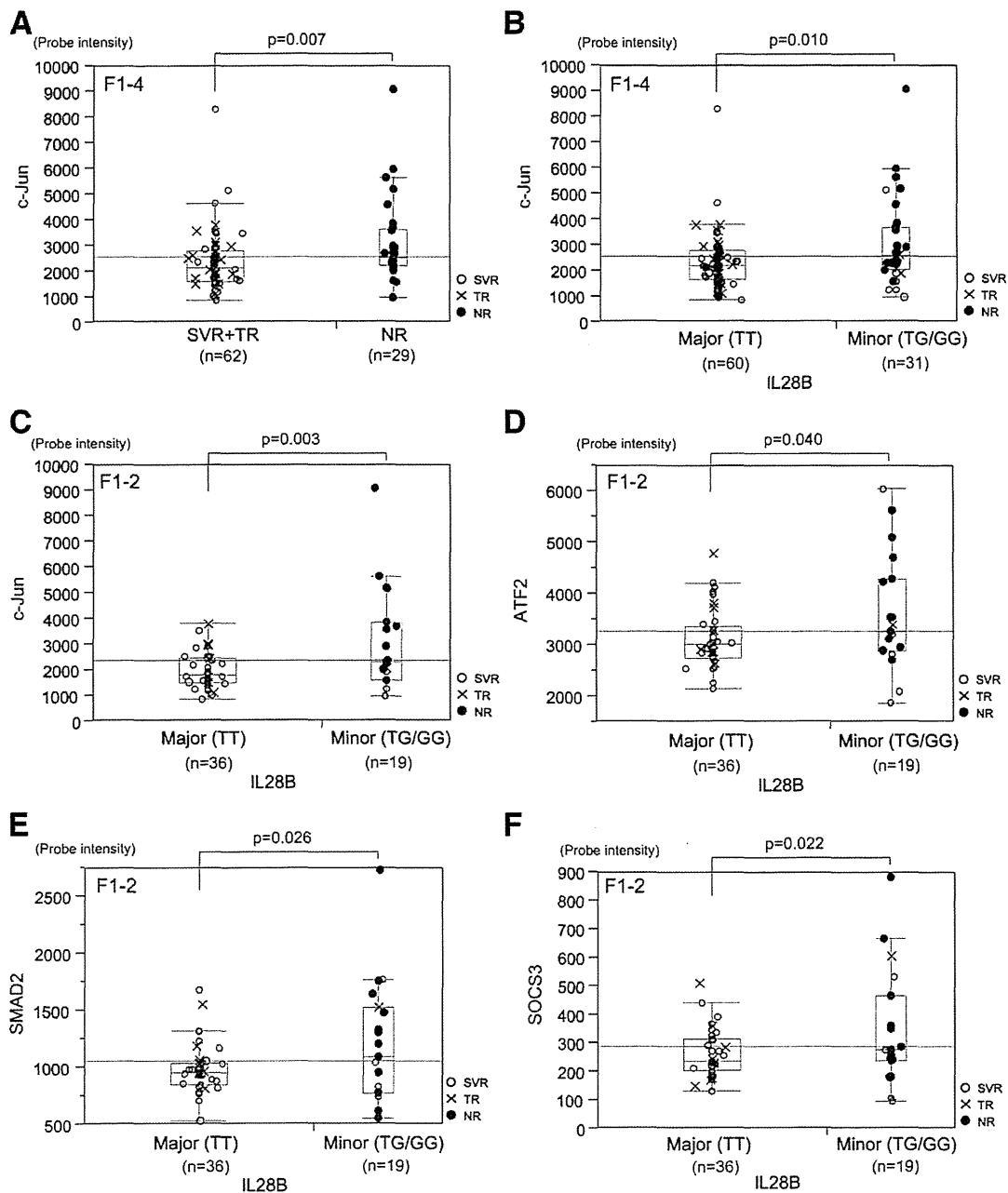
Fig. 6. Relationship between TGF-β signaling and treatment response and the IL28B genotype. The expression of c-Jun was up-regulated in NR (A) and IL28B minor genotype (TG/GG at rs8099917) (B) patients in all fibrosis stages (F1-4). The expression of ATF2 (D), Smad2 (E), and Socs3 (F) was up-regulated in IL28B minor genotype (TG/GG at rs8099917) patients at early fibrosis stages (F1-2).

(TG/GG at rs8099917) than in those with the treatment-sensitive IL28B major genotype (TT) (Fig. 6B).[5] Interestingly, TGF-β signaling was more activated in patients with the treatment-resistant IL28B minor genotype at an early stage of liver fibrosis (F1 and F2). The expression of c-Jun, ATF2, Smad2, and Socs3 was significantly higher in IL28B minor genotype patients (Fig. 6C-F).

BCAAs Inhibit TGF-β Signaling and Restore IFN Signaling. Previously, we reported that BCAAs restored IFN signaling in the amino acid-depleted condition (1/5 DMEM) by activating mTORC1 signaling and suppressing Foxo3a-Socs3 signaling.[6] In the present study, we examined whether BCAAs could inhibit TGF-β signaling and restore IFN signaling. Western
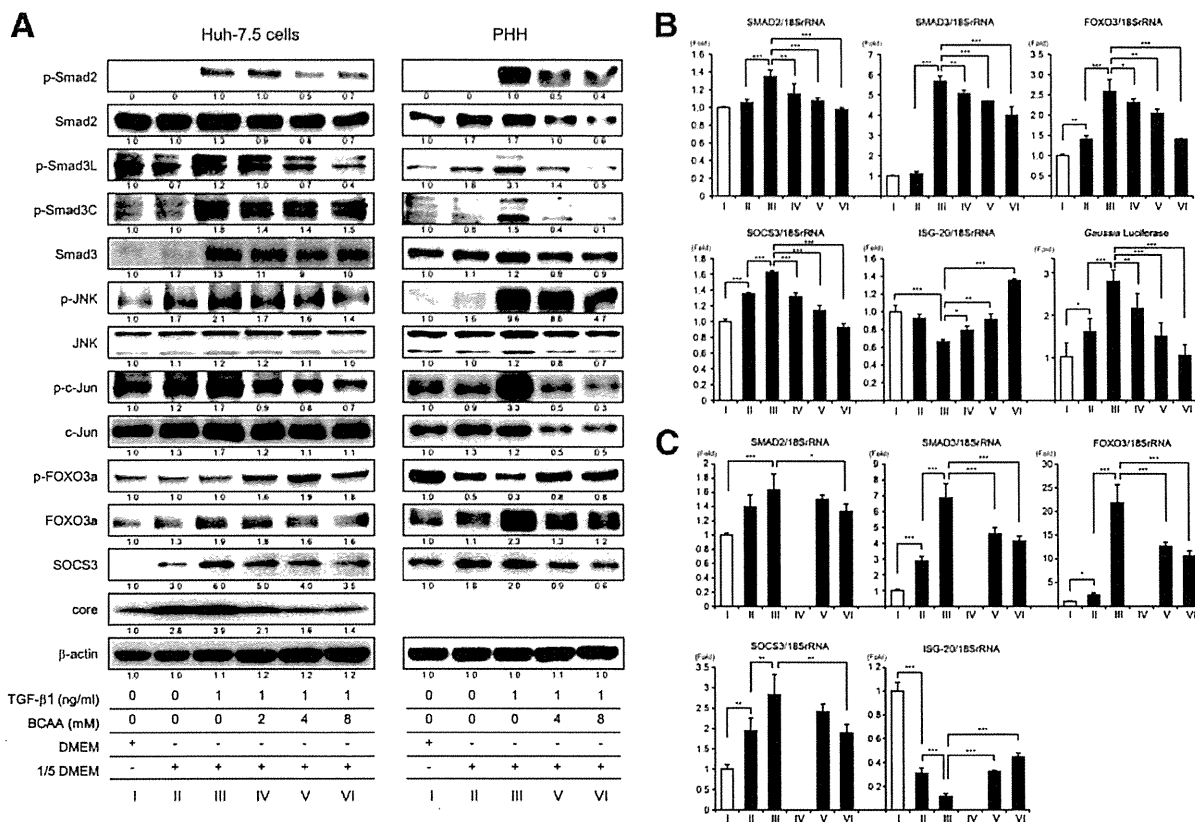
Fig. 7. BCAAs inhibit the effect of malnutrition and TGF-β signaling in Huh-7.5 cells and PHH. A: Western blotting of TGF-β and Foxo3a-Socs3 signaling in Huh-7.5 HCV (+) and PHH treated with amino acid depletion (1/5 DMEM), TGF-β1, and BCAAs. B,C: mRNA expression of TGF-β, Foxo3a-Socs3, and IFN signaling in Huh-7.5 HCV (+) (B) and PHH (C) treated with amino acid depletion (1/5 DMEM), TGF-β1, and BCAA.

blotting analysis showed that BCAAs dose-dependently repressed the expression of p-Smad3L, p-Smad3C, p-JNK, p-c-Jun, Foxo3a, Socs3 (in Huh-7.5 cells and PHH), and HCV core protein (in Huh-7.5 cells), which was induced by amino acid depletion (1/5 DMEM) and TGF-β1 treatment (Fig. 7A). RTD-PCR demonstrated similar mRNA expression patterns (Smad2, Smad3, Foxo3a, and Socs3a) to those obtained by western blotting (Fig. 7B,C), and BCAAs induced the expression of ISG-20 (in Huh-7.5 cells and PHH) and decreased HCV replication in a dose-dependent manner (in Huh-7.5 cells) (Fig. 7B). These results were also confirmed in HCVcc HJ3-5-infected Huh-7 cells (Supporting Fig. 6).

BCAAs and TGF-β RI Potentiate the Anti-HCV Activity of DAAs. Finally, we examined whether BCAAs or TGF-β RI potentiate the anti-HCV activity of DAAs. Amino acid depletion (1/5 DMEM) and TGF-β1 treatment significantly increased HCV replication (deduced from *Gaussia* luciferase activity), and BCAAs (8 mM) and boceprevir (250 nM; NS3 protease inhibitor) inhibited HCV replication to 64% and 50%, respec-

tively (Fig. 8A, black bars). The combination of BCAAs (8 mM) and boceprevir (250 nM) further inhibited HCV replication to 10% and canceled the effect of amino acid depletion (1/5 DMEM) and TGF-β1 treatment, which supported HCV replication (Fig. 8A, compare white and black bars). Similarly, TGF-β RI (10 μM) repressed HCV replication to 60%, and its combination with boceprevir (250 nM) decreased HCV replication to 16% (Fig. 8B, black bars) and canceled the effect of amino acid depletion (1/5 DMEM) and TGF-β1 treatment (Fig. 8A, compare white and black bars). Thus, BCAAs and TGF-β RI had an additive effect on the anti-HCV activity of boceprevir and would be useful for CH-C patients with advanced fibrosis and the IL28B treatment-resistant genotype. A similar effect was obtained by using the NS5A inhibitor BMS-790052; however, its effect was less than that of boceprevir (Supporting Fig. 7).

Discussion

The recently developed DAAs have significantly improved the efficacy of anti-HCV therapy. Triple
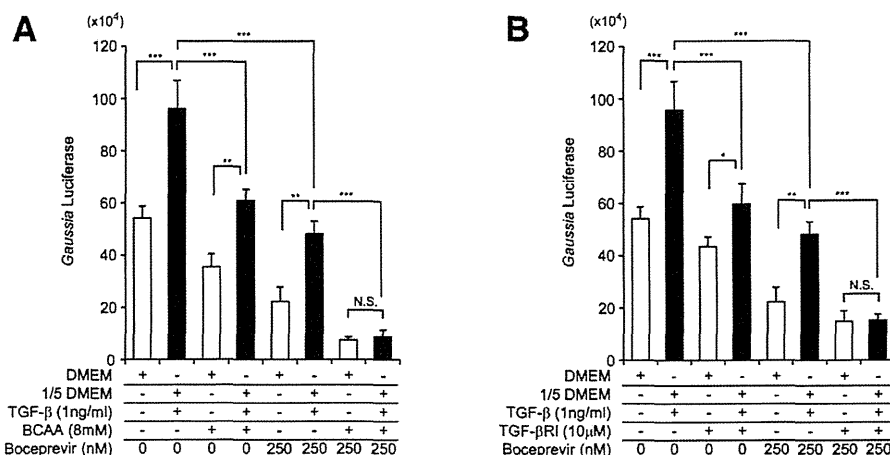
Fig. 8. Anti-HCV activity of boceprevir in combination with BCAAs (A) and TGF-β1 RI (B). HCV replication in Huh-7.5 cells was deduced by *Gaussia* luciferase activity. Boceprevir in combination with BCAAs (A) and TGF-β1 RI (B) efficiently repressed HCV replication in Huh-7.5 cells treated with amino acid depletion (1/5 DMEM) and TGF-β1. The experiments were performed in triplicate and repeated 3 times (*$P < 0.05$, **$P < 0.01$, ***$P < 0.001$).

therapy comprising PEG-IFN, RBV, and DAA (e.g., telaprevir or boceprevir) has significantly increased SVR rates; however, its efficacy is poor in difficult-to-cure patients such as those with cirrhosis and the IL28B treatment-resistant genotype.[2,4] An IFN-free regimen using a combination of DAAs would be effective to treat these difficult-to-cure patients; however, the emergence of multiple drug resistant viruses and the high cost of these therapies should be considered carefully in the future. Therefore, standard PEG-IFN plus RBV combination therapy is still useful as an alternative therapy for CH-C.

Previously, we reported that malnutrition in patients with the advanced fibrosis stage of CH-C is associated with IFN resistance and impaired IFN signaling by inhibiting mTORC1 and activating Socs3-mediated IFN inhibitory signaling through the nutrition-sensing transcriptional factor Foxo3a.[6] However, the effect of profibrosis signaling on IFN signaling was not addressed in our previous study. In the present study, using clinical samples and cell lines, we clearly showed that TGF-β signaling inhibits IFN signaling by activating Foxo3a-Socs3-mediated IFN inhibitory signaling (Figs. (1 and 4)) and inhibiting mTORC1 signaling (Fig. 5).

Using Foxo3a promoter-luciferase reporter constructs, we showed that TGF-β1 activated Foxo3a promoter activity through an AP1 transcription factor binding site. Among the components of AP1, c-Jun and probably ATF2, but not c-Fos, were involved in this induction. Previous reports showed that c-Jun and ATF2 were induced by amino acid depletion[13,14] and

TGF-β1 treatment,[15,16] although the induction of c-Jun by amino acid depletion was not obvious in PHH in this study. It could be considered that malnutrition and profibrotic signaling cooperatively activated the Foxo3a promoter through the AP1 site and that c-Jun induction was more specifically regulated by TGF-β1 in normal hepatocytes. Mutation of the AP1 binding site (pGL4-FOXO3a [-1340-MT]) abolished the response to amino acid depletion (1/5 DMEM) and TGF-β1 treatment (Fig. 3E; Supporting Fig. 2). Conversely, c-Jun overexpression combined with amino acid depletion (1/5 DMEM) and TGF-β1 treatment activated the Foxo3a promoter by 32-fold (Fig. 3F). In addition, we showed that TGF-β1 inhibited mTORC1 signaling, as demonstrated by the decreased expression of RHEB, p-mTOR, and p-p70S6K (Fig. 5A).

These results were in concordance with gene expression in the liver of CH-C patients. The expression of c-Jun and ATF2 was significantly correlated with Smad2 and Foxo3a expression, respectively (Fig. 4), while the expression of RHEB was significantly negatively correlated with Smad2 expression in the liver of CH-C patients (Fig. 5C). In this study, TGF-β1 and TGF-β2 expression was up-regulated in advanced liver fibrosis, and the expression of TGF-β2 was well correlated with the downstream signaling molecule Smad2 (Fig. 1B-D). Although we could not address the biological differences in TGF-β isoforms in this study, TGF-β1 and TGF-β2 reportedly mediate a similar signaling pathway to induce profibrotic responses.[17] Collectively, TGF-β signaling inhibited IFN signaling by activating Foxo3a-Socs3 IFN inhibitory signaling and

inhibiting mTORC1-IFN stimulating signaling *in vitro* and *in vivo*. Recently, Lee et al. showed that Foxo3a regulates the TGF-β1 promoter directly.[18] Combining their data and ours, there must be positive feedback regulation between TGF-β1 and Foxo3a. Moreover, they identified a polymorphism in Foxo3a (rs12212067: T > G) in which the minor (G) allele was involved in the increased production of TGF-β1 and associated with the inflammatory response.[18] We genotyped the Foxo3a rs12212067 polymorphism in three cell lines and observed TT in Huh-7 and Huh-7.5 and GG in TTNT (Supporting Table 3). Although we could not find a significant difference in Foxo3a promoter activity in response to TGF-β1 among these cell lines (Supporting Fig. 2), further studies should be performed to compare Foxo3a-Socs3 IFN inhibitory signaling among them. Furthermore, it is worthwhile to examine the relationship between the genotype at rs12212067 and treatment response and severity of liver disease in CH-C patients in the future.

Another interesting finding in this study was that TGF-β signaling was related to the IL28B genotype (Fig. 6). The expression of c-Jun was significantly higher in IL28B treatment-resistant minor genotype (TG/GG at rs8099917) patients than in IL28B treatment-sensitive major genotype (TT) patients. Moreover, the expression of c-Jun, Smad2, ATF2, and Socs3 was up-regulated more in IL28B minor genotype patients than in IL28B major genotype patients, especially in those with early stage liver fibrosis (F1-2). The underlying mechanisms of these findings are not known so far; however, we recently reported that the noncanonical WNT signaling ligand WNT5A is up-regulated in the liver of IL28B minor genotype patients and plays a role in treatment resistance.[19] WNT5A reportedly mediates downstream signaling through c-Jun and ATF2 in *Xenopus* cells and human osteosarcoma cells.[20,21] It could be speculated that WNT5A potentiates TGF-β signaling through these transcription factors, although this hypothesis should be tested in the future.

We examined whether BCAAs and TGF-β RI improve the IFN inhibitory signaling induced by malnutrition and TGF-β signaling (Fig. 7). Previously, we demonstrated that BCAAs improved the IFN signaling that was inhibited by malnutrition.[6] In the present study, we found that BCAAs blocked TGF-β signaling by decreasing the levels of p-Smad3L, p-JNK, and c-Jun (Fig. 7A). Consequently, BCAAs decreased the expression of Foxo3a, Socs3, and HCV core protein (Fig. 7). In addition, we found that the combination of BCAAs or TGF-β RI and the NS3 protease inhibi-

tor boceprevir efficiently inhibited HCV replication and canceled the positive effects of malnutrition and TGF-β1 on HCV replication (Fig. 8). A recent report showed that the NS3 protease of HCV mimics TGF-β2 and activates the TGF-β type I receptor.[22] Therefore, the anti-HCV effect of boceprevir could be potentiated in combination with BCAAs or TGF-β RI, which blocked TGF-β signaling and increased IFN signaling. Therefore, the combination of BCAAs or TGF-β RI with DAAs could be useful for the treatment of difficult-to-cure CH-C patients with advanced liver fibrosis and the IL28B treatment-resistant genotype.

In conclusion, we clarified that TGF-β signaling inhibits IFN signaling and is related to the treatment-resistant phenotype of CH-C patients with advanced liver fibrosis and the IL28B treatment-resistant genotype. Furthermore, blocking TGF-β signaling by BCAAs or TGF-β RI could potentiate the anti-HCV effect of DAAs. An oral TGF-β RI small compound, LY2157299, is now being assessed in a phase II trial for the treatment of advanced-stage HCC. Further studies should be performed to address the significance of these compounds for the eradication of HCV in patients with advanced liver fibrosis for preventing HCC.

Author Contributions: Takayoshi Shirasaki performed most experiments and drafted the article; Masao Honda, study design, interpretation of data, and drafting of the article; Tetsuro Shimakami, HCV replication analysis and cellular experiments; Kazuhisa Murai, HCV replication analysis and cellular experiments; Takayuki Shiomoto, HCV replication analysis and cellular experiments; Hikari Okada, HCV replication analysis and cellular experiments; Riuta Takabatake, HCV replication analysis and cellular experiments; Akihiro Tokumaru, HCV replication analysis and cellular experiments; Yoshio Sakai, acquisition of clinical data; Taro Yamashita, acquisition of clinical data; Stanley M. Lemon, study design and interpretation of data; Seishi Murakami, study design and interpretation of data; Shuichi Kaneko, study concept and design.

References

1. Yoshida H, Shiratori Y, Moriyama M, Arakawa Y, Ide T, Sata M, et al. Interferon therapy reduces the risk for hepatocellular carcinoma: national surveillance program of cirrhotic and noncirrhotic patients with chronic hepatitis C in Japan IHIT Study Group. Inhibition of Hepatocarcinogenesis by Interferon Therapy. Ann Intern Med 1999;131:174-181.

2. Trembling PM, Tanwar S, Rosenberg WM, Dusheiko GM. Treatment decisions and contemporary versus pending treatments for hepatitis C. Nat Rev Gastroenterol Hepatol 2013;10:713-728.

3. Hezode C, Fontaine H, Dorival C, Larrey D, Zoulim F, Canva V, et al. Triple therapy in treatment-experienced patients with HCV-cirrhosis in a multicentre cohort of the French Early Access Programme (ANRS CO20-CUPIC) – NCT01514890. J Hepatol 2013;59:434-441.

4. Bruno S, Vierling JM, Esteban R, Nyberg LM, Tanno H, Goodman Z, et al. Efficacy and safety of boceprevir plus peginterferon-ribavirin in patients with HCV G1 infection and advanced fibrosis/cirrhosis. J Hepatol 2013;58:479-487.

5. Tanaka Y, Nishida N, Sugiyama M, Kurosaki M, Matsuura K, Sakamoto N, et al. Genome-wide association of IL28B with response to pegylated interferon-alpha and ribavirin therapy for chronic hepatitis C. Nat Genet 2009;41:1105-1109.

6. Honda M, Takehana K, Sakai A, Tagata Y, Shirasaki T, Nishitani S, et al. Malnutrition impairs interferon signaling through mTOR and FoxO pathways in patients with chronic hepatitis C. Gastroenterology 2011;141:128-140.

7. Okitsu T, Kobayashi N, Jun HS, Shin S, Kim SJ, Han J, et al. Transplantation of reversibly immortalized insulin-secreting human hepatocytes controls diabetes in pancreatectomized pigs. Diabetes 2004;53:105-112.

8. Honda M, Nakamura M, Tateno M, Sakai A, Shimakami T, Shirasaki T, et al. Differential interferon signaling in liver lobule and portal area cells under treatment for chronic hepatitis C. J Hepatol 2010;53:817-826.

9. Yi M, Ma Y, Yates J, Lemon SM. Compensatory mutations in E1, p7, NS2, and NS3 enhance yields of cell culture-infectious intergenotypic chimeric hepatitis C virus. J Virol 2007;81:629-638.

10. Eferl R, Wagner EF. AP-1: a double-edged sword in tumorigenesis. Nat Rev Cancer 2003;3:859-868.

11. Bai X, Ma D, Liu A, Shen X, Wang QJ, Liu Y, et al. Rheb activates mTOR by antagonizing its endogenous inhibitor, FKBP38. Science 2007;318:977-980.

12. Carayol N, Katsoulidis E, Sassano A, Altman JK, Druker BJ, Platanias LC. Suppression of programmed cell death 4 (PDCD4) protein expression by BCR-ABL-regulated engagement of the mTOR/p70 S6 kinase pathway. J Biol Chem 2008;283:8601-8610.

13. Chaveroux C, Jousse C, Cherasse Y, Maurin AC, Parry L, Carraro V, et al. Identification of a novel amino acid response pathway triggering

ATF2 phosphorylation in mammals. Mol Cell Biol 2009;29:6515-6526.

14. Fu L, Balasubramanian M, Shan J, Dudenhausen EE, Kilberg MS. Auto-activation of c-JUN gene by amino acid deprivation of hepatocellular carcinoma cells reveals a novel c-JUN-mediated signaling pathway. J Biol Chem 2011;286:36724-36738.

15. Sano Y, Harada J, Tashiro S, Gotoh-Mandeville R, Maekawa T, Ishii S. ATF-2 is a common nuclear target of Smad and TAK1 pathways in transforming growth factor-beta signaling. J Biol Chem 1999;274: 8949-8957.

16. Mu Y, Gudey SK, Landstrom M. Non-Smad signaling pathways. Cell Tissue Res 2012;347:11-20.

17. Leask A, Abraham DJ. TGF-beta signaling and the fibrotic response. FASEB J 2004;18:816-827.

18. Lee JC, Espeli M, Anderson CA, Linterman MA, Pocock JM, Williams NJ, et al. Human SNP links differential outcomes in inflammatory and infectious disease to a FOXO3-regulated pathway. Cell 2013;155:57-69.

19. Honda M, Shirasaki T, Shimakami T, Sakai A, Horii R, Arai K, et al. Hepatic interferon-stimulated genes are differentially regulated in the liver of chronic hepatitis C patients with different interleukin 28B genotypes. HEPATOLOGY 2014;59:828-838.

20. Yamanaka H, Moriguchi T, Masuyama N, Kusakabe M, Hanafusa H, Takada R, et al. JNK functions in the non-canonical Wnt pathway to regulate convergent extension movements in vertebrates. EMBO Rep 2002;3:69-75.

21. Yamagata K, Li X, Ikegaki S, Oneyama C, Okada M, Nishita M, et al. Dissection of Wnt5a-Ror2 signaling leading to matrix metalloproteinase (MMP-13) expression. J Biol Chem 2012;287:1588-1599.

22. Sakata K, Hara M, Terada T, Watanabe N, Takaya D, Yaguchi S, et al. HCV NS3 protease enhances liver fibrosis via binding to and activating TGF-beta type I receptor. Sci Rep 2013;3:3243.

Supporting Information

Additional Supporting Information may be found in the online version of this article at the publisher's website.

nature medicine

Regulation of the hepatitis C virus RNA replicase by endogenous lipid peroxidation

Daisuke Yamane[1,2], David R McGivern[1,2], Eliane Wauthier[2,3], MinKyung Yi[4], Victoria J Madden[5], Christoph Welsch[6], Iris Antes[7], Yahong Wen[8], Pauline E Chugh[2,9], Charles E McGee[10], Douglas G Widman[11], Ichiro Misumi[10], Sibali Bandyopadhyay[12,13], Seungtaek Kim[1,2,14], Tetsuro Shimakami[1,2], Tsunekazu Oikawa[2,3], Jason K Whitmire[2,9,10], Mark T Heise[2,10], Dirk P Dittmer[2,9], C Cheng Kao[8], Stuart M Pitson[15], Alfred H Merrill Jr[12,13], Lola M Reid[2,3] & Stanley M Lemon[1,2,9]

Oxidative tissue injury often accompanies viral infection, yet there is little understanding of how it influences virus replication. We show that multiple hepatitis C virus (HCV) genotypes are exquisitely sensitive to oxidative membrane damage, a property distinguishing them from other pathogenic RNA viruses. Lipid peroxidation, regulated in part through sphingosine kinase-2, severely restricts HCV replication in Huh-7 cells and primary human hepatoblasts. Endogenous oxidative membrane damage lowers the 50% effective concentration of direct-acting antivirals in vitro, suggesting critical regulation of the conformation of the NS3-4A protease and the NS5B polymerase, membrane-bound HCV replicase components. Resistance to lipid peroxidation maps genetically to transmembrane and membrane-proximal residues within these proteins and is essential for robust replication in cell culture, as exemplified by the atypical JFH1 strain of HCV. Thus, the typical, wild-type HCV replicase is uniquely regulated by lipid peroxidation, providing a mechanism for attenuating replication in stressed tissue and possibly facilitating long-term viral persistence.

Reactive oxygen species (ROS) are an unavoidable byproduct of aerobic metabolism and a double-edged sword for complex cellular systems[1]. Although central to many disease states, ROS also function as second messengers during embryonic development and, in macrophages, contribute to host defense against infection[2,3]. Viral infections frequently induce ROS generation, either by stimulating host immune responses or by direct tissue injury[4]. HCV, a hepatotropic RNA virus with a unique capacity for persistence[5], induces substantial intrahepatic oxidative stress, thereby promoting liver injury[6,7]. Limited data suggest that lipid peroxidation restricts HCV replication[8], but how it impairs the viral replicative machinery is unknown.

Although HCV is a leading cause of cirrhosis and liver cancer[5], many details of its replication remain obscure, as most HCV strains replicate poorly in cell culture. A notable exception is JFH1, a genotype 2a virus recovered from a patient with fulminant hepatitis[9]. JFH1 recapitulates the entire virus life cycle and replicates efficiently in Huh-7 hepatoma cells[9–11]. In recent years, it has become a laboratory standard used in most studies of HCV replication. However, there is

very limited understanding of the robust replication phenotype that sets it apart from other HCVs[12,13].

Like all positive-strand RNA virus genomes, the HCV genome is synthesized by a multiprotein replicase complex that assembles in association with intracellular membranes. Known as the 'membranous web' in HCV-infected cells[14,15], this specialized cytoplasmic compartment provides a platform for viral RNA synthesis. Its membranes are enriched in cholesterol, sphingolipids and phosphatidylinositol-4-phosphate[16,17]. Assembly of the membranous web involves recruitment of phosphatidylinositol-4-phosphate-3 kinase and annexin A2 (refs. 17–19) and possibly also direct membrane remodeling by nonstructural HCV proteins[20]. Whereas lipid metabolism also plays key roles in later steps in the virus life cycle[21], these modifications of intracellular membranes are closely linked to viral RNA synthesis.

Sphingolipids are increased in abundance within the replicase membranes and are important factors in HCV replication[22–25]. Sphingomyelin interacts with and in some genotypes stimulates NS5B, the viral RNA-dependent RNA polymerase[23,26]. While studying

[1]Department of Medicine, Division of Infectious Diseases, The University of North Carolina at Chapel Hill, Chapel Hill, North Carolina, USA. [2]Lineberger Comprehensive Cancer Center, The University of North Carolina at Chapel Hill, Chapel Hill, North Carolina, USA. [3]Department of Cell Biology and Physiology, The University of North Carolina at Chapel Hill, Chapel Hill, North Carolina, USA. [4]Department of Microbiology and Immunology, University of Texas Medical Branch, Galveston, Texas, USA. [5]Department of Pathology, The University of North Carolina at Chapel Hill, Chapel Hill, North Carolina, USA. [6]Department of Internal Medicine I, J.W. Goethe University Hospital, Frankfurt, Germany. [7]Center for Integrated Protein Science Munich (CIPSM), Department of Life Sciences, Technical University Munich, Freising, Germany. [8]Department of Molecular and Cellular Biochemistry, Indiana University, Bloomington, Indiana, USA. [9]Department of Microbiology and Immunology, The University of North Carolina at Chapel Hill, Chapel Hill, North Carolina, USA. [10]Department of Genetics, The University of North Carolina at Chapel Hill, Chapel Hill, North Carolina, USA. [11]Department of Epidemiology, The University of North Carolina at Chapel Hill, Chapel Hill, North Carolina, USA. [12]School of Biology, Georgia Institute of Technology, Atlanta, Georgia, USA. [13]Parker H. Petit Institute for Bioengineering and Bioscience, Georgia Institute of Technology, Atlanta, Georgia, USA. [14]Severance Biomedical Science Institute, Yonsei University College of Medicine, Seoul, Korea. [15]Centre for Cancer Biology, SA Pathology, Adelaide, South Australia, Australia. Correspondence should be addressed to D.Y. (yamane@email.unc.edu) or S.M.L. (smlemon@med.unc.edu).

these virus-host interactions in cell culture, we discovered that JFH1 differs from other HCV strains in its response to inhibitors of sphingolipid-converting enzymes. These initial observations led to experiments that show the HCV replicase to be exquisitely sensitive to endogenous lipid peroxidation, a feature lacking in the atypical JFH1 strain and other pathogenic RNA viruses. Our findings suggest that HCV possesses a unique capacity to sense lipid peroxides induced by infection and to respond to their presence by restricting viral RNA synthesis, thereby limiting virus replication and possibly facilitating virus persistence.

RESULTS

Sphingosine kinase-2 regulates HCV replication

We determined how inhibitors of sphingolipid-converting enzymes influence replication of three cell culture–adapted HCVs: H77S.3, a genotype 1a virus, N2, a genotype 1b virus, and HJ3-5, an intergenotypic chimera expressing the genotype 2a JFH1 replicase. To assess replication, we monitored *Gaussia princeps* luciferase (GLuc) produced by Huh-7.5 cells transfected with synthetic viral RNAs containing in-frame GLuc insertions[27] (**Fig. 1a**). Unexpectedly, the H77S.3/GLuc and HJ3-5/GLuc RNAs demonstrated contrary responses to many inhibitors, including, most notably, SKI, a sphingosine kinase (SPHK) inhibitor (**Fig. 1b** and **Supplementary Fig. 1a,b**). We also observed contrasting responses to sphingolipid supplementation (**Supplementary Fig. 1c**). SKI (1 µM) enhanced replication of H77S.3/GLuc and also N2/GLuc by three- to sixfold but suppressed replication of HJ3-5/GLuc (**Fig. 1b,c**). These effects were evident within 48 h of exposure. We observed similar effects with viral RNAs lacking GLuc insertions: SKI enhanced H77S.3 protein expression tenfold while slightly suppressing HJ3-5 protein expression (**Fig. 1d**). Thus, changes in the cellular environment induced by SKI favor H77S.3 and N.2 replication and inhibit that of HJ3-5. These effects were not due to altered cell proliferation or viral RNA

translation (**Supplementary Fig. 2a,b**). We observed similar results with autonomously replicating, subgenomic HCV RNAs ('replicons') in multiple cell types (**Supplementary Fig. 2c,d**).

SPHK is expressed as two isoforms[28], which we individually silenced by transfecting cells with gene-specific siRNAs. Partial type 2 SPHK (SPHK2) depletion enhanced replication of H77S.3/GLuc and N.2/GLuc, whereas SPHK1 depletion inhibited both viruses (**Fig. 1e,f**). In contrast, replication of HJ3-5/GLuc and cell culture–adapted JFH1 (JFH-QL/GLuc, **Fig. 1a**) viruses was increased following SPHK1 depletion and decreased after SPHK2 knockdown. Neither SPHK1 nor SPHK2 knockdown substantially affected cell proliferation (**Supplementary Fig. 2e**). Thus, SKI enhances replication of H77S.3/GLuc and N.2/GLuc by inhibiting SPHK2. Consistent with this, SKI preferentially inhibited SPHK2 in cell-free assays (**Supplementary Fig. 2f**) and demonstrated no activity against endogenous SPHK1 at low concentrations (≤2 µM) (**Supplementary Fig. 2g**). SKI did not act by regulating the intracellular abundance of sphingomyelin, cholesterol, triglyceride or lipid droplets, and sensitivity to SKI was not determined by the sphingomyelin binding domain of NS5B (**Supplementary Results** and **Supplementary Figs. 3 and 4**).

Lipid peroxidation is a key factor in SKI regulation of HCV

Polyunsaturated fatty acids (PUFAs) inhibit replication of genotype 1b HCV replicons by inducing lipid peroxidation[8,29]. Notably, although PUFAs such as arachidonic acid, docosahexaenoic acid or linoleic acid potently suppressed H77S.3/GLuc replication without affecting cell viability, HJ3-5/GLuc was highly resistant to this inhibitory effect (**Fig. 2a,b** and **Supplementary Fig. 5a,b**). Thus, PUFAs appear to phenocopy the effect of SPHK2 on HCV replication, suggesting that SPHK2 promotes lipid peroxidation. Consistent with this hypothesis, SKI completely abolished the inhibitory effects of PUFAs on H77S.3/GLuc and N.2/GLuc (**Fig. 2c**). SKI also lowered the intracellular abundance of malondialdehyde (MDA), a secondary product

Figure 1 SKI enhances genotype 1 HCV replication while suppressing JFH1-based viruses by inhibiting SPHK2. (a) HCV RNA genomes that express GLuc fused to foot-and-mouth disease virus 2A autoprotease as part of the HCV polyprotein. Arrowheads indicate cell culture–adaptive mutations. (b) Left, dose-response effects of SKI on replication of H77S.3/GLuc (red) or HJ3-5/GLuc (blue) RNAs in Huh-7.5 cells. Right, effect of 1 µM SKI on replication of H77S.3 (red) or HJ3-5 (blue) RNAs. Data represent relative amounts of GLuc secreted between 48–72 h (left) or intracellular RNA levels at 72 h (right). *P < 0.05, **P < 0.001 by two-way ANOVA. (c) Effect of 1 µM SKI on GLuc activities of the indicated viruses presented as fold change from baseline (6 h). *P < 0.05, **P < 0.001 by two-way ANOVA. (d) Flow cytometric analysis of NS5A expression in Huh-7.5 cells electroporated with H77S.3 or HJ3-5 RNA and treated with 1 µM SKI or DMSO. (e,f) Effect of siRNAs targeting SPHK isoforms or nontargeting control siRNA on replication of different HCV RNAs (e) and protein abundance of each SPHK isoform (f). LU, light units. *P < 0.05, **P < 0.01 by two-way ANOVA. Results represent the mean ± s.e.m. from two independent (b,c,d) or triplicate (e) experiments.
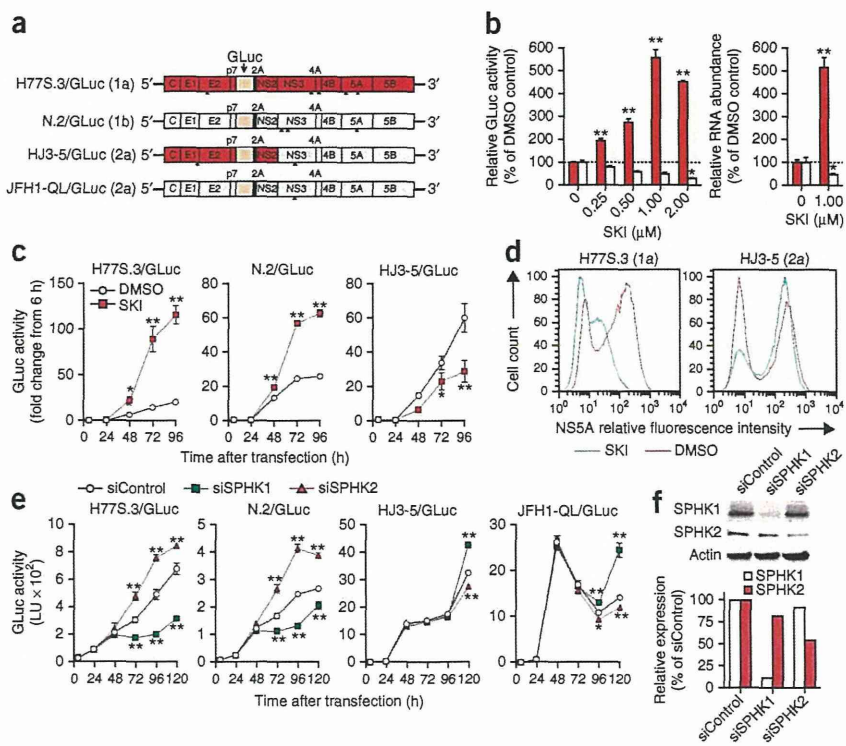
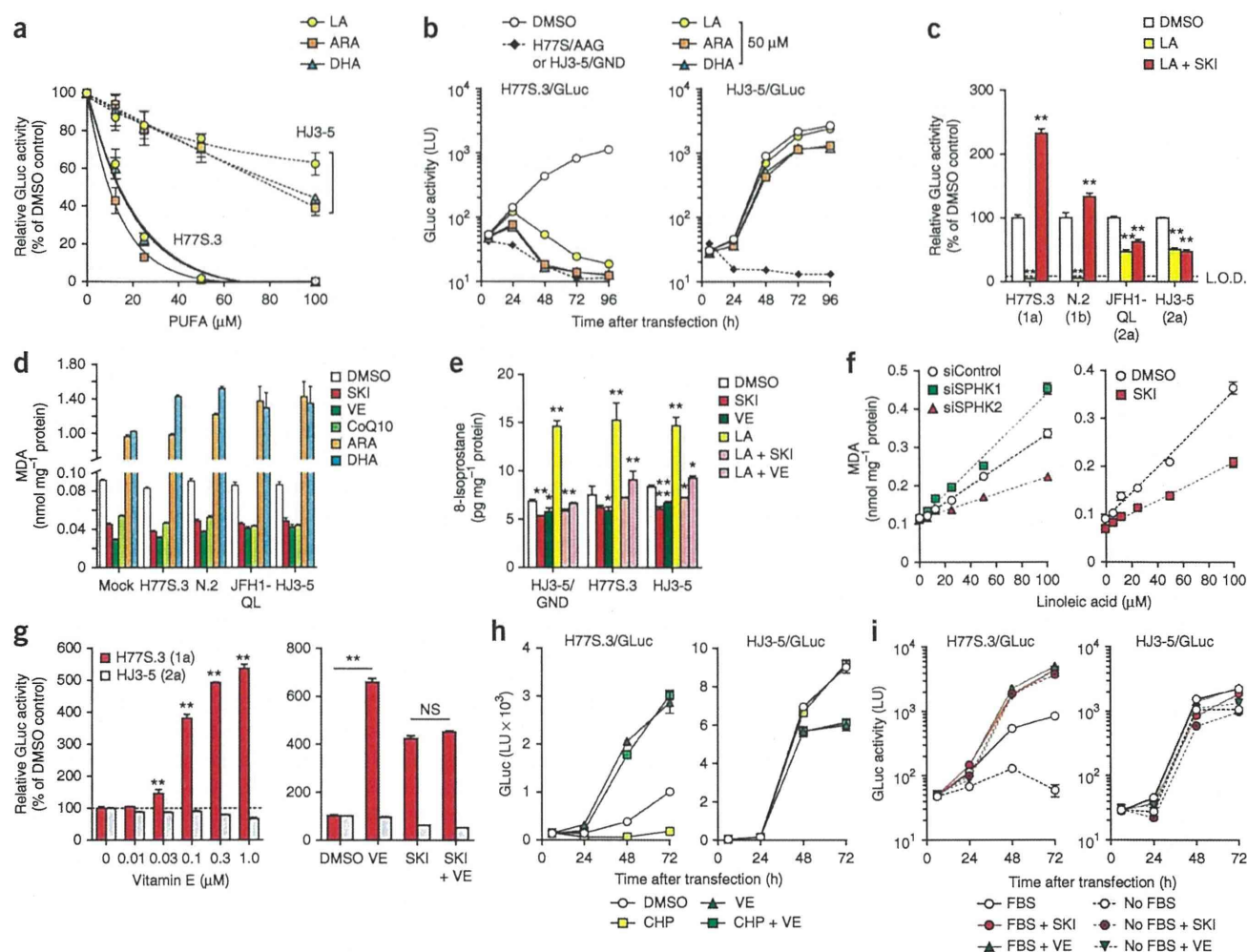**Figure 2** Differential regulation of HCV strains by SPHK2-mediated lipid peroxidation. (**a**) Dose-dependent effects of PUFAs on H77S.3/GLuc and HJ3-5/GLuc RNAs in Huh-7.5 cells. Data represent percentage secreted GLuc activity between 48–72 h relative to DMSO control. (**b**) Growth kinetics of H77S.3/GLuc and HJ3-5/GLuc RNAs in the presence of 50 μM PUFAs. Data are mean ± s.e.m. of GLuc activity in supernatant fluids of two replicate cultures. (**c**) Cells transfected with HCV RNAs encoding GLuc treated with DMSO, 100 μM linoleic acid (LA) or 100 μM linoleic acid plus 1 μM SKI. Data represent percentage secreted GLuc activity between 48–72 h relative to DMSO control. L.O.D., limit of detection. (**d**) Effect of 1 μM SKI, 1 μM vitamin E (VE), 100 μM CoQ10 or 50 μM arachidonic acid (ARA) or docosahexaenoic acid (DHA) on intracellular MDA abundance in cells transfected with the indicated HCV/GLuc RNAs at 72 h. MDA was significantly increased by PUFAs and reduced by SKI or lipophilic antioxidants (*P* < 0.01 by ANOVA). (**e**) Analysis of 8-isoprostane abundance in cells electroporated with the indicated HCV RNAs and grown in the presence of 1 μM SKI or vitamin E or of 50 μM linoleic acid with or without 1 μM SKI or vitamin E for 48 h. (**f**) Left, effect of siRNA targeting SPHK isoforms (**Fig. 1f**) on MDA accumulation after treatment with increasing concentrations of linoleic acid (6.25, 12.5, 25, 50, 100 μM) for 24 h. Right, MDA levels in Huh-7.5 cells treated with increasing concentrations of linoleic acid in the presence of DMSO or 1 μM SKI. (**g**) Effects of increasing concentrations of vitamin E (left) or 1 μM vitamin E alone or 1 μM vitamin E plus 1 μM SKI (right) on replication of H77S.3/GLuc and HJ3-5/GLuc RNAs. Data represent GLuc secreted between 48–72 h relative to DMSO control. NS, not significant. (**h**) GLuc secretion from Huh-7.5 cells transfected as in **a** and treated with 10 μM CHP with or without 10 μM vitamin E. (**i**) Influence of SKI or vitamin E (each 1 μM) on replication of H77S.3 and HJ3-5 viruses expressing GLuc in cells cultured in the presence or absence of 10% FBS. Data represent mean ± s.e.m. from two (**a–f,i**) or three (**g,h**) independent experiments. *P* < 0.05, **P* < 0.01 by two-way ANOVA.

of peroxidative degradation, in both HCV-infected and uninfected cells (**Fig. 2d**). SKI was as effective as the lipophilic antioxidants vitamin E (α-tocopherol) and coenzyme Q10 (CoQ10) in reducing MDA abundance and, like vitamin E and CoQ10, prevented large increases in lipid peroxidation induced by PUFAs (**Fig. 2d,e**). SKI also reduced both endogenous and PUFA-induced synthesis of 8-isoprostane, an alternative biomarker of lipid peroxidation (**Fig. 2e**). Conversely, RNAi-mediated depletion of SPHK1 increased the intracellular abundance of MDA in cells treated with increasing concentrations of linoleic acid, whereas SPHK2 knockdown, like SKI, reduced it (**Fig. 2f**). Thus, the contrasting

effects of SPHK1 and SPHK2 on HCV replication may be explained by their opposing actions on peroxidation of endogenous PUFA. These results identify SPHK2 as a key mediator of lipid peroxidation.

Lipid-soluble antioxidants, including multiple forms of vitamin E (α-, *rac*-β- and γ-tocopherols), CoQ10 and butylated hydroxytoluene, enhanced H77S.3/GLuc replication in a concentration-dependent fashion, as described for a genotype 1b replicon[8], but suppressed HJ3-5/GLuc replication (**Fig. 2g** and **Supplementary Fig. 5c–e**). Notably, the effects of vitamin E and SKI on H77S.3/GLuc or N.2/GLuc replication were not additive (**Fig. 2g** and **Supplementary Fig. 5f**), suggesting